

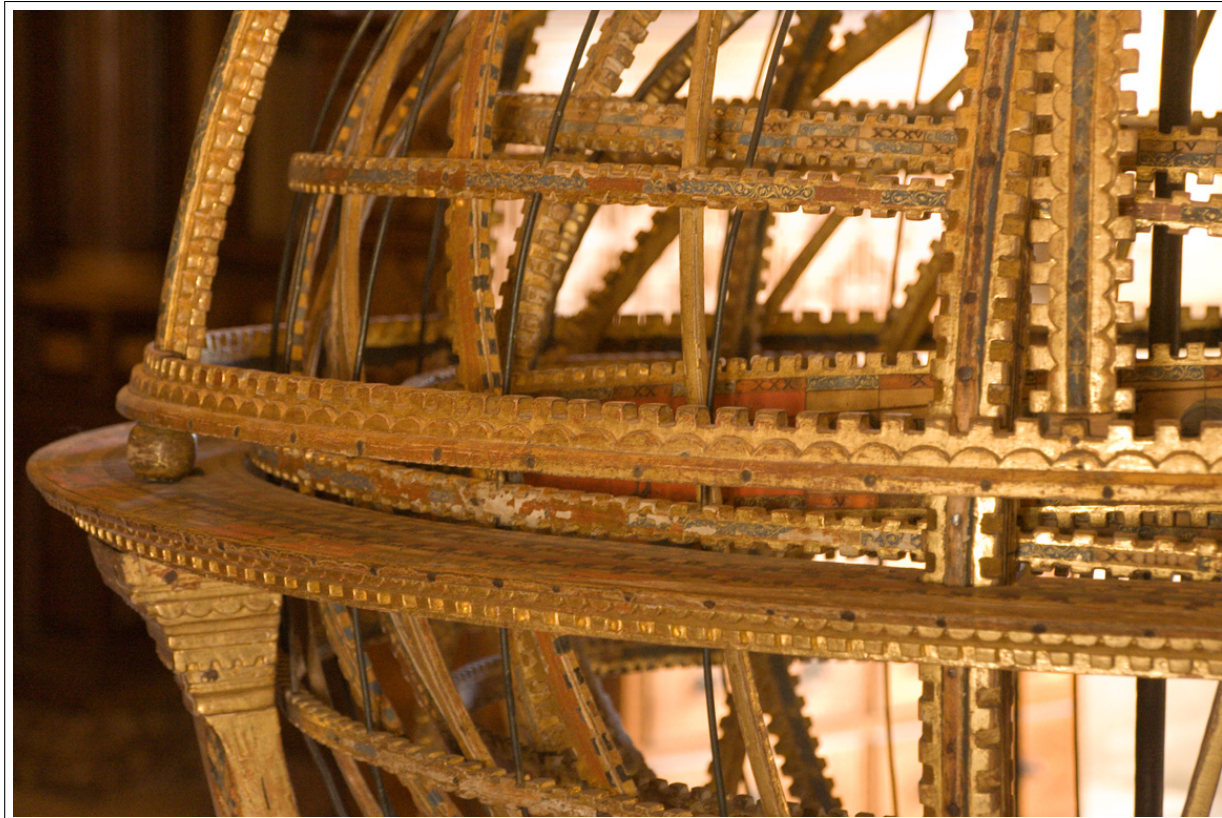
# SCAMP

*v1.20*

User's guide

E. BERTIN  
Institut d'Astrophysique de Paris

February 19, 2014





# Contents

|          |  |           |
|----------|--|-----------|
| <b>1</b> | <b>What is SCAMP?</b>                        | <b>1</b>  |
| <b>2</b> | <b>Skeptical Sam's questions</b>             | <b>1</b>  |
| <b>3</b> | <b>License</b>                               | <b>2</b>  |
| <b>4</b> | <b>Installing the software</b>               | <b>2</b>  |
| 4.1      | Obtaining SCAMP . . . . .                    | 2         |
| 4.2      | Software and hardware requirements . . . . . | 2         |
| 4.3      | Installation . . . . .                       | 3         |
| <b>5</b> | <b>Using SCAMP</b>                           | <b>3</b>  |
| 5.1      | Input files . . . . .                        | 3         |
| 5.1.1    | Catalogues . . . . .                         | 3         |
| 5.1.2    | “.ahead” header files . . . . .              | 4         |
| 5.2      | Output files . . . . .                       | 4         |
| 5.2.1    | “.head” header files . . . . .               | 4         |
| 5.2.2    | Output catalogues . . . . .                  | 5         |
| 5.2.3    | Diagnostic files . . . . .                   | 5         |
| 5.3      | The Configuration file . . . . .             | 5         |
| 5.3.1    | Creating a configuration file . . . . .      | 5         |
| 5.3.2    | Format of the configuration file . . . . .   | 5         |
| 5.3.3    | Configuration parameter list . . . . .       | 6         |
| <b>6</b> | <b>How SCAMP works</b>                       | <b>17</b> |
| 6.1      | Overview of the software . . . . .           | 17        |
| 6.2      | Parallel processing . . . . .                | 17        |
| 6.3      | Loading data . . . . .                       | 18        |
| 6.3.1    | Preparing good input catalogues . . . . .    | 18        |
| 6.3.2    | Filtering detections . . . . .               | 20        |
| 6.4      | Sorting the catalogues . . . . .             | 20        |
| 6.4.1    | Field groups . . . . .                       | 20        |
| 6.4.2    | Astrometric instruments . . . . .            | 21        |
| 6.4.3    | Photometric instruments . . . . .            | 22        |
| 6.5      | Pre-processing of mosaics . . . . .          | 22        |
| 6.6      | Astrometric reference catalogues . . . . .   | 23        |

|           |  |           |
|-----------|--|-----------|
| 6.7       | Matching with the reference catalogues . . . . .         | 24        |
| 6.7.1     | Finding the pixel scale and the position angle . . . . . | 26        |
| 6.7.2     | Finding the coordinate shift . . . . .                   | 27        |
| 6.7.3     | Image flipping . . . . .                                 | 27        |
| 6.7.4     | Refining the matching procedure . . . . .                | 28        |
| 6.7.5     | Performance of the matching procedure . . . . .          | 29        |
| 6.8       | Cross-identification . . . . .                           | 29        |
| 6.9       | Astrometric solution . . . . .                           | 29        |
| 6.9.1     | Principle . . . . .                                      | 29        |
| 6.9.2     | Balancing the constraints . . . . .                      | 32        |
| 6.9.3     | Taking care of outliers . . . . .                        | 33        |
| 6.10      | Photometric solution . . . . .                           | 34        |
| 6.11      | Photometric measurements . . . . .                       | 34        |
| 6.11.1    | Principle . . . . .                                      | 34        |
| 6.12      | Differential chromatic refraction . . . . .              | 35        |
| <b>7</b>  | <b>Merged output catalogue</b>                           | <b>36</b> |
| <b>8</b>  | <b>Full output catalogue</b>                             | <b>36</b> |
| <b>9</b>  | <b>Examples</b>  | <b>37</b> |
| 9.1       | Example 1 . . . . .                                      | 37        |
| 9.2       | Example 2 . . . . .                                      | 38        |
| <b>10</b> | <b>Troubleshooting</b>                                   | <b>38</b> |
| <b>11</b> | <b>Acknowledging SCAMP</b>                               | <b>39</b> |
| <b>12</b> | <b>Acknowledgements</b>                                  | <b>39</b> |



## 1 What is SCAMP?

SCAMP (Software for Calibrating AstroMetry and Photometry) is a program that computes astrometric projection parameters from source catalogues derived from FITS images. The computed solution is expressed according to the WCS standard<sup>1</sup>. The main features of SCAMP are:

- Compatibility with SExtractor FITS or Multi-Extension-FITS catalogue format in input,
- Generation of WCS-compliant and SWARP-compatible FITS image headers in output,
- Automatic grouping of catalogues on the sky
- Selectable on-line astrometric reference catalogue
- Automatic determination of scale, position angle, flipping and coordinate shift using fast pattern-matching
- Several astrometric calibration modes for single detectors and detector arrays
- Combined astrometric solutions for multi-channel/instrument surveys
- Highly configurable astrometric distortion polynomials
- Correction for differential chromatic refraction
- Proper motion measurements
- Multi-threaded code to take advantage of multiple processors.
- XML VOTable-compliant output of meta-data.

## 2 Skeptical Sam's questions

Skeptical Sam doesn't have time to test software extensively but is always keen on asking aggressive questions to the author to find out if a program could fit his needs.

**S.Sam:** So there is a new astrometric software. What are the main differences with software which exists already?

**Author:** The most useful feature of SCAMP is undoubtedly its ability to deal in a quasi-optimum way with a large number of overlapping observations, and it can provide robust calibrations even with poorly devised survey strategies. SCAMP was designed from the ground up to work with CCD mosaics. Finally, SCAMP is particularly fast and easy to use.

**S.Sam:** What is the link between SCAMP, SExtractor and SWARP?

**Author:** SCAMP reads SExtractor catalogues and produces FITS-like image headers that SWARP can read and use for image stacking.

**S.Sam:** What typical astrometric precision may I expect from the calibration provided by SCAMP?

---

<sup>1</sup>see <http://www.cv.nrao.edu/fits/documents/wcs/wcs.html>

**Author:** If the instrument on which the observations have been conducted is geometrically “fair” enough, the internal accuracy of the calibration is often limited by photon-noise. An RMS precision of a few hundredths of a pixel is quite common. Add a blurb about atmospheric noise. The “global” astrometric accuracy is another story, and nowadays it is largely limited by the precision of astrometric reference catalogues.

## 3 License

SCAMP is free software: you can redistribute it and/or modify it under the terms of the GNU General Public License as published by the Free Software Foundation, either version 3 of the License, or (at your option) any later version. SCAMP is distributed in the hope that it will be useful, but WITHOUT ANY WARRANTY; without even the implied warranty of MERCHANTABILITY or FITNESS FOR A PARTICULAR PURPOSE. See the GNU General Public License for more details. You should have received a copy of the GNU General Public License along with SCAMP. If not, see <http://www.gnu.org/licenses/>.

## 4 Installing the software

### 4.1 Obtaining SCAMP

The easiest way to obtain SCAMP is to download it from the official website<sup>2</sup>, or alternatively from the current official anonymous FTP site<sup>3</sup>. At this address the latest versions of the program are available as standard `.tar.gz` Unix source archives as well as documentation and RPM binary packages for various architectures.

### 4.2 Software and hardware requirements

SCAMP has been developed on Unix machines (GNU/Linux), and should compile on any POSIX-compliant system, provided that the following libraries/packages have been installed:

- ATLAS V3.6 and above<sup>4</sup> (<http://math-atlas.sourceforge.net/>)
- CDSCLIENT V3.4 and above (<http://cdsweb.u-strasbg.fr/doc/cdsclient.html>)
- FFTw V3.0 and above<sup>5</sup> (<http://www.fftw.org/>)
- PLPLOT V5.9 and above (<http://www.plplot.org/>)

PLPLOT is only required for producing diagnostic plots. Note that ATLAS and FFTw are not necessary for the binary versions of SCAMP which include these libraries statically linked.

The software is run in (ANSI) text-mode from a shell. A window system is necessary only when PLPLOT is used in interactive mode.

---

<sup>2</sup><http://astromatic.net/software/scamp>

<sup>3</sup>[ftp://ftp.iap.fr/pub/from\\_users/bertin/scamp/](ftp://ftp.iap.fr/pub/from_users/bertin/scamp/)

<sup>4</sup>Use the `--with-atlas` and/or `--with-atlas-incdir` options to specify the ATLAS library and include paths if the software is installed at unusual locations.

<sup>5</sup>If you install it from the source package, please make sure to compile FFTW with the `configure` options `--enable-threads --enable-float`).

The amount of memory required depends mostly on the size of the input catalogues and on the number  $N_{\text{ast}}$  of exposures and astrometric "contexts" (stable instruments) involved in the astrometric solution. This amounts to about 140 bytes per detection in the input catalogues, plus a few tens of kbytes for every FITS table. To this one should add the memory space used by the normal equation matrix, which is  $8 \times N_{\text{T}}^2$  bytes, with, in the default SCAMP configuration,

$$N_{\text{T}} = N_{\text{ast}} \times N_{\text{arr}} \times N_{\text{p}} + (N_{\text{exp}} - N_{\text{ast}}) \times 6, \quad (1)$$

where  $N_{\text{arr}}$  is the number of focal plane arrays (extensions) in each exposure,  $N_{\text{p}}$  the number of polynomial terms of the solution (20 for a 3<sup>rd</sup> polynomial in  $x$  and  $y$ ), and  $N_{\text{exp}}$  the number of exposures. Actually one should probably double the memory space used by the normal equation matrix to account for buffers in the ATLAS library. It is not uncommon to see memory usage amounting to a few gigabytes when millions of detections are involved. **Add a concrete example with  $N_{\text{ast}} > 1$ .**

### 4.3 Installation

To install, you must first uncompress and unarchive the archive:

```
gzip -dc scamp-x.x.tar.gz | tar xvf -
```

A new directory called `scamp-x.x` should now appear at the current position on your disk. You should then just enter the directory and follow the instructions in the file called "INSTALL".

## 5 Using SCAMP

SCAMP is run from the shell with the following syntax:

```
% scamp Catalog1 [Catalog2 ...] [@Catalog_list1 [@Catalog_list2 ...]] -c configuration-file
    [-Parameter1 Value1] [- Parameter2Value2 ...]
```

The part enclosed within brackets is optional. The file names of input catalogues can be directly provided in the command-line, or in lists, preceded with '@'. Lists are ASCII files containing the input file names (one per line). One should use lists instead of the catalogue file names if the number of input catalogues is too large to be handled directly by the shell. Any "-Parameter Value" statement in the command-line overrides the corresponding definition in the configuration-file or any default value (see below).

### 5.1 Input files

#### 5.1.1 Catalogues

Catalogue files read by SCAMP must be in SExtractor "FITS\_LDAC" binary format. It is strongly advised to use SExtractor version 2.4.4 or later. The catalogues *must* contain all the following parameters in order to perform the calibration:

- Centroid coordinates. These are defined by the `CENTROID_KEYS` configuration parameter (default: `XWIN_IMAGE` and `YWIN_IMAGE`).
- Centroid errors. These are defined by the `CENTROIDERR_KEYS` configuration parameter (default: `ERRAWIN_IMAGE`, `ERRBWIN_IMAGE` and `ERRTHETAWIN_IMAGE`).

- Astrometric distortion factors. These are defined by the DISTORT\_KEYS configuration parameter (default: XWIN\_IMAGE and YWIN\_IMAGE).
- Flux measurements. These are defined by the PHOTFLUX\_KEY configuration parameter (default: FLUX\_AUTO).
- Flux errors. These are defined by the PHOTFLUXERR\_KEY configuration parameter (default: FLUXERR\_AUTO).

In addition, it is advised (but not mandatory) to include optional SExtractor catalogue fields:

- FLAGS, FLAGS\_WEIGHT and/or IMAFLAGS\_ISO to filter out blended and corrupted detections.
- FLUX\_RADIUS: to identify small glitches or extended objects.

### 5.1.2 “.ahead” header files

The binary catalogues in “FITS\_LDAC” format read by SCAMP contain a copy of the original FITS image headers. These headers provide fundamental information such as frame dimensions, World Coordinate System (WCS) data and many other FITS keywords which SCAMP uses to derive a full astrometric and photometric calibration. It is often needed to change or add keywords in some headers. Editing FITS files is not convenient, so SCAMP provides read (and write) support for “external” header files. External headers may either be real FITS header cards (no carriage-return), or ASCII files containing lines in FITS-like format, with the final line starting with “END\_\_\_\_\_”. Multiple extensions must be separated by an “END\_\_\_\_\_” line. External “headers” need not contain all the FITS keywords normally required. The keywords present in external headers are only there to override their counterparts in the original image headers or to add new ones.

Hence for every input (say, `xxxx.cat`) FITS catalogue, SCAMP looks for a `xxxx.ahead` header file, loads it if present, and overrides or adds to image header keywords those found there. `.ahead` is the default suffix; it can be changed using the AHEADER\_SUFFIX configuration parameter.

Some cases require one or several keywords to be added/modified in *all* input catalogues. SCAMP offers the possibility to put these keywords in one single external header file , which will be read before all other .ahead files (but after reading the catalogue headers). The name of this file is `scamp.ahead` by default; it can be changed using the AHEADER\_GLOBAL configuration parameter. [show an example of a typical .ahead file](#)

## 5.2 Output files

### 5.2.1 “.head” header files

SCAMP itself generates FITS header keywords, containing updated astrometric and photometric information. These keywords are written in ASCII to external header files, with the `.head` filename extension by default (the suffix can be changed with the HEADER\_SUFFIX configuration parameter). In combination with the original image files, these `.head` headers are ready to be used by the SWARP image stacking tool<sup>6</sup>.

The astrometric engine at the heart of SCAMP and SWARP is based on M. Calabretta’s *WCSlab* library<sup>7</sup>, to which we added the handling of polynomial distortion parameters (FITS keywords

---

<sup>6</sup><http://astromatic.net/software/swarp>

<sup>7</sup>Available at <http://www.cv.nrao.edu/fits/src/wcs/>

`PV_xx_xx`) as proposed in one of the earlier WCS documents<sup>8</sup>. All celestial coordinate computations are performed in the equatorial system, although galactic or ecliptic coordinates are supported in input and output.

### 5.2.2 Output catalogues

SCAMP can save two kinds of catalogues: local copies of the reference catalogues downloaded from the Vizier server (see §6.6), and a “merged”, calibrated version of input catalogues (§7).

### 5.2.3 Diagnostic files

Two types of files can be generated by SCAMP, providing diagnostics about the calibrations:

- “Check-plots” are graphic charts generated by SCAMP, showing scatter plots or calibration maps. The `CHECKPLOT_TYPE` and `CHECKPLOT_NAME` configuration parameters allow the user to provide a list of check-plot types and file names, respectively. A variety of raster and vector file formats, from JPEG to Postscript, can be set with `CHECKPLOT_DEV`. PNG is the default. See the `CHECKPLOT` section of §5.3.3 for details.
- An XML file providing a processing summary and various statistics in VOTable format is written if the `WRITE_XML` switch is set to Y (the default). The `XML_NAME` parameter can be used to change the default file name `scamp.xml`. The XML file can be displayed with any recent web browser; the XSLT stylesheet installed together with SCAMP will automatically translate it into a dynamic, user-friendly web-page. For more advanced usages (e.g. access from a remote web server), alternative XSLT translation URLs may be specified using the `XSL_URL` configuration parameter.

## 5.3 The Configuration file

Each time SCAMP is run, it looks for a configuration file. If no configuration file is specified in the command-line, it is assumed to be called “`scamp.conf`” and to reside in the current directory. If no configuration file is found, SCAMP will use its own internal default configuration.

### 5.3.1 Creating a configuration file

SCAMP can generate an ASCII dump of its internal default configuration, using the “`-d`” option. By redirecting the standard output of SCAMP to a file, one creates a configuration file that can easily be modified afterward:

```
% scamp -d >default.scamp
```

A more extensive dump with less commonly used parameters can be generated by using the “`-dd`” option.

### 5.3.2 Format of the configuration file

The format is ASCII. There must be only one parameter set per line, following the form:

---

<sup>8</sup><http://www.cv.nrao.edu/fits/documents/wcs/wcs.html>

*Config-parameter*      *Value(s)*

Extra spaces or linefeeds are ignored. Comments must begin with a “#” and end with a linefeed. Values can be of different types: strings (can be enclosed between double quotes), floats, integers, keywords or Boolean (Y/y or N/n). Some parameters accept zero or several values, which must then be separated by commas. Values separated by commas, spaces, tabs or linefeeds may also be read from an ASCII file if what is given is a filename preceded with @ (e.g. @values.txt). Integers can be given as decimals, in octal form (preceded by digit 0), or in hexadecimal (preceded by 0x). The hexadecimal format is particularly convenient for writing multiplexed bit values such as binary masks. Environment variables, written as \$HOME or \${HOME} are expanded.

### 5.3.3 Configuration parameter list

Here is a list of all the parameters known to SCAMP. Please refer to next section for a detailed description of their meaning. Some “advanced” parameters (indicated with an asterisk) are also listed. They must be used with caution, and may be rescoped or removed without notice in future versions.

|  |   |          |
|--|---|----------|
| AHEADER_GLOBAL*  | scamp.ahead   | string   |
| Name of a global input header file read for all input catalogues <i>before</i> other .ahead files.   |   |          |
| AHEADER_SUFFIX   | .ahead  | string   |
| Filename extension for additional input headers.   |   |          |
| AIRMASS_KEY  | AIRMASS   | string   |
| FITS header keyword that stores the airmass. Set to 1.0 if not found.  |   |          |
| ASTR_ACCURACY*   | 0.01  | float    |
| Default additional astrometric uncertainty parameter, used if keyword indicated by ASTRACCURACY_KEY is not found in FITS catalogue header. |   |          |
| ASTRACCURACY_KEY*  | ASTRACCU  | string   |
| FITS header keyword that stores the astrometric additional uncertainty parameter. Use ASTR_ACCURACY if not found.                          |   |          |
| ASTRACCURACY_TYPE*   | SIGMA-PIXEL   | keywords |
| Type of additional component of astrometric uncertainties:   |   |          |
| SIGMA-PIXEL  | Constant component added in quadrature, described by its standard deviation in pixels     |          |
| SIGMA-ARCSEC   | Constant component added in quadrature, described by its standard deviation in arcseconds |          |

|                   |  |                 |
|-------------------|--|-----------------|
| TURBULENCE-ARCSEC | Exposure time, seeing and field-of-view dependent “turbulence” component added in quadrature, scaled by $\sigma_0$ , which corresponds to the amplitude (in arcsec) of pairwise random motion at $10'$ in a one second exposure taken from the ground. $\sigma_0$ depends on the observing site and conditions, but not on wavelength, or telescope diameter. $\sigma_0 = 0.054''$ , as reported by Han & Gatewood (1995) for Mauna Kea, seems appropriate for the best observing sites. |                 |
| ASTRCLIP_NSIGMA*  | 3.0  | <i>float</i>    |
|                   | Clipping boundary for the second astrometric pass, in units of standard deviation.   |                 |
| ASTREF_CATALOG    | USNO-B1  | <i>keywords</i> |
|                   | Reference catalogue for astrometry (see Table 1):  |                 |
| NONE              | No reference   |                 |
| CMC-14            | Carlsberg Meridian Catalog number 14   |                 |
| FILE              | Local file(s) provided   |                 |
| DENIS-3           | DEep Near Infrared Survey catalogue version 3  |                 |
| USNO-A1           | US Naval Observatory catalogue version A1  |                 |
| USNO-A2           | US Naval Observatory catalogue version A2  |                 |
| USNO-B1           | US Naval Observatory catalogue version B1  |                 |
| GSC-1.3           | Guide Star Catalog V1.3  |                 |
| GSC-2.2           | Guide Star Catalog V2.2  |                 |
| GSC-2.3           | Guide Star Catalog V2.3  |                 |
| NOMAD-1           | Naval Observatory Merged Astrometric Dataset version 1   |                 |
| PPMX              | Position and Proper Motions eXtended   |                 |
| SDSS-R3           | Sloan Digital Sky Survey release 3   |                 |
| SDSS-R5           | Sloan Digital Sky Survey release 5   |                 |
| SDSS-R6           | Sloan Digital Sky Survey release 6   |                 |
| SDSS-R7           | Sloan Digital Sky Survey release 7   |                 |
| SDSS-R8           | Sloan Digital Sky Survey release 8   |                 |
| SDSS-R9           | Sloan Digital Sky Survey release 9   |                 |
| 2MASS             | 2MASS near-infrared catalogue  |                 |
| TYCHO-2           | Tycho-2 catalogue of the 2.5 million brightest stars   |                 |
| UCAC-1            | USNO CCD Astrograph Catalog version 1  |                 |
| UCAC-2            | USNO CCD Astrograph Catalog version 2  |                 |
| UCAC-3            | USNO CCD Astrograph Catalog version 3  |                 |
| UCAC-4            | USNO CCD Astrograph Catalog version 4  |                 |
| ASTREF_WEIGHT*    | 1.0  | <i>float</i>    |

Weight correction factor to apply to the sources for tightening or loosening the astrometric solution with respect to the reference catalogue(s).

|                           |   |                       |
|---------------------------|---|-----------------------|
| <b>ASTREF_BAND</b>        | <b>DEFAULT</b>  | <i>string</i>         |
|                           | Name of the filter passband to use in astrometric reference catalogue, or <b>DEFAULT</b> for default, <b>BLUEST</b> or <b>REDDEST</b> for the passband with the shortest or largest effective wavelength, respectively. |                       |
| <b>ASTREFCAT_NAME*</b>    | <b>astrefcat.cat</b>  | <i>strings</i>        |
|                           | File names of local astrometric reference catalogues (active if <b>ASTREF_CATALOG</b> is set to <b>FILE</b> ), through which SCAMP will browse to find astrometric reference stars.                                     |                       |
| <b>ASTREFCENT_KEYS*</b>   | <b>X_WORLD, Y_WORLD</b>   | <i>strings</i>        |
|                           | Names of the columns, in the local astrometric reference catalogue(s), that contain the centroid coordinates in degrees. Active only if <b>ASTREF_CATALOG</b> is set to <b>FILE</b> .                                   |                       |
| <b>ASTREFERR_KEYS*</b>    | <b>ERRA_WORLD, ERRB_WORLD, ERRTHETA_WORLD</b>   | <i>strings</i>        |
|                           | Names of the columns, in the local astrometric reference catalogue(s), that contain the major and minor axes and position angle of the error ellipses. Active only if <b>ASTREF_CATALOG</b> is set to <b>FILE</b> .     |                       |
| <b>ASTREFMAG_KEY*</b>     | <b>MAG</b>  | <i>string</i>         |
|                           | Name of the column, in the local astrometric reference catalogue(s), that contains the catalogue magnitudes. Active only if <b>ASTREF_CATALOG</b> is set to <b>FILE</b> .   |                       |
| <b>ASTREFMAGERR_KEY*</b>  | <b>MAGERR</b>   | <i>string</i>         |
|                           | Name of the optional column, in the local astrometric reference catalogue(s), that contains the catalogue magnitude uncertainties. Active only if <b>ASTREF_CATALOG</b> is set to <b>FILE</b> .                         |                       |
| <b>ASTREFOBSDATE_KEY*</b> | <b>OBSDATE</b>  | <i>string</i>         |
|                           | Name of the optional column, in the local astrometric reference catalogue(s), that contains observation dates. Active only if <b>ASTREF_CATALOG</b> is set to <b>FILE</b> .   |                       |
| <b>ASTREFMAG_LIMITS</b>   | <b>-99.0, 99.0</b>  | <i>floats (n = 2)</i> |
|                           | Allowed magnitude range for sources in the astrometric reference catalogue.   |                       |
| <b>ASTRINSTRU_KEY</b>     | <b>FILTER, QRUNID</b>   | <i>strings</i>        |
|                           | FITS header keyword(s) that define the astrometric context: catalogues with identical values for the <b>ASTRINSTRU_KEY</b> keyword(s) are assumed to originate from the same “astrometric instrument”.                  |                       |
| <b>CDSCLIENT_EXEC</b>     | <b>/usr/local/bin/aclient.cgi</b>   | <i>string</i>         |
|                           | Filename of the CDSclient executable used for astrometric reference catalogue requests. See <a href="http://cdsweb.u-strasbg.fr/doc/cdsclient.html">http://cdsweb.u-strasbg.fr/doc/cdsclient.html</a> .                 |                       |
| <b>CENTROID_KEYS</b>      | <b>XWIN_IMAGE, YWIN_IMAGE</b>   | <i>strings</i>        |

SExtractor measurements used as source centroids in the input catalogues.

**CHECKPLOT\_ANTIALIAS\***      Y      Boolean  
If true (Y), PBM, PNG and JPEG check-plots are generated with anti-aliasing. IMAGEMAGICK's convert tool must be installed. See <http://www.imagemagick.org>.

| CHECKPLOT_DEV  | XWIN                                     | <i>keywords</i> |
|--|--|-----------------|
| PLPlot devices to be used for check-plots (see PLPlot documentation for more details): |  |                 |
| NULL   | No output                                |                 |
| XWIN   | X-Window                                 |                 |
| TK   | Tk window (if available)                 |                 |
| PLMETA   | PLPlot .plm meta-file                    |                 |
| PS   | Black-and-white .ps Postscript file      |                 |
| PSC  | Colour .ps Postscript file               |                 |
| XFIG   | XFig .fig vector file                    |                 |
| PNG  | Portable Network Graphics .png image     |                 |
| JPEG   | JPEG .jpg image                          |                 |
| PSTEX  | PSTeX (a variant of Postscript) .ps file |                 |
| PDF  | Portable Document Format .pdf file       |                 |
| SVG  | Scalable Vector Graphics .svg file       |                 |

CHECKPLOT\_NAME fgroups, distort, strings  
astr\_interror2d, astr\_interror1d,  
astr\_referror2d, astr\_referror1d, astr\_chi2,  
phot\_error

File names for each series of check-plots. SCAMP will automatically insert field group or instrument number, and append/replace filename extensions with the appropriate ones, depending on the chosen `CHECKPLOT_DEV`(s) (.png for PNG files, .jpg for JPEG, etc.).

CHECKPLOT\_TYPE FGROUPS, DISTORTION,,  
ASTR\_INTERRO2D, ASTR\_INTERRO1D,  
ASTR\_REFERROR1D, ASTR\_REFERROR1D, ASTR\_CHI2,  
PHOT\_ERROR

Diagnostic check-plots to generate during SCAMP processing (SCAMP must have been configured without the `--without-plplot` option):

|                                 |   |
|---------------------------------|---|
| <code>NONE</code>               | No plot   |
| <code>SKY_ALL</code>            | All sky chart showing the position of input frames and groups on the celestial sphere using an Aitoff projection.   |
| <code>FGROUPS</code>            | Sky charts showing, for each group, frame limits, detections and astrometric sources after astrometric calibration.   |
| <code>DISTORTION</code>         | Chart showing for each astrometric instrument an astrometric model of the input frame(s) after calibration. The pixel size is represented over the field of view using a colour scale ranging from blue to red.                           |
| <code>ASTR_INTERROR1D</code>    | Scatter plot showing the (internal, 1-dimensional) pairwise differences between coordinates of overlapping detections as a function of position along each reprojected axis.  |
| <code>ASTR_INTERROR2D</code>    | 2-dimensional scatter plot showing the (internal) pairwise differences between coordinates of overlapping detections.   |
| <code>ASTR_REFERROR1D</code>    | Scatter plot showing the 1-dimensional differences between detection coordinates and coordinates of the associated astrometric reference stars as a function of position along each reprojected axis.                                     |
| <code>ASTR_REFERROR2D</code>    | 2-dimensional scatter plot showing the differences between detection coordinates and coordinates of the associated astrometric reference star.  |
| <code>ASTR_PIXERROR1D</code>    | Scatter plot showing the (internal, 1-dimensional) differences between coordinates of individual overlapping detections and the average ones as a function of position along each detector axis.  |
| <code>ASTR_SUBPIXERROR1D</code> | Scatter plot showing the (internal, 1-dimensional) differences between coordinates of individual overlapping detections and the average ones as a function of position within the pixel along each detector axis.                         |
| <code>ASTR_CHI2</code>          | internal and reference $\chi^2$ per degree of freedom of the astrometric solution as a function of catalogue sequence number.   |
| <code>ASTR_REFSYSMAP</code>     | 2-dimensional vector plot of residual systematics of detection coordinates with respect to the reference catalogue coordinates, for a given astrometric instrument.   |
| <code>ASTR_REFPROPER</code>     | Proper motions derived from the input catalogues as a function of proper motions from the reference catalogue (when available).   |
| <code>ASTR_COLSHIFT1D</code>    | Scatter plot showing the (internal, 1-dimensional) pairwise differences between coordinates of overlapping detections as a function of colour index along each reprojected axis (one subplot per combination of photometric instruments). |

|                        |   |  |
|------------------------|---|--|
| ASTR_XPIXERROR2D       | Chart of weighted-average residuals of source pixel $x$ coordinates for the current instrument, with respect to the average celestial position from all instruments, back-projected onto the current instrument's pixel coordinate system.                |  |
| ASTR_YPIXERROR2D       | Chart of weighted-average residuals of source pixel $y$ coordinates for the current instrument, with respect to the average celestial position from all instruments, back-projected onto the current instrument's pixel coordinate system.                |  |
| PHOT_ERROR             | Scatter plot showing for each photometric instrument the (internal) pairwise magnitude differences between overlapping detections as a function of position along each reprojected axis.  |  |
| PHOT_ERRORVSMAG        | Scatter plot showing for each photometric instrument the (internal) pairwise magnitude differences between overlapping detections as a function of magnitude.   |  |
| PHOT_ZPCORR            | Photometric zero-point correction computed by SCAMP as a function of catalogue sequence number (one sub-plot per photometric instrument).   |  |
| PHOT_ZPCORR3D          | Photometric zero-point correction computed by SCAMP as a function of position in the group (one sub-plot per photometric instrument).   |  |
| SHEAR_VS_AIRMASS       | Scatter plot showing the field contraction (aspect ratio) as a function of airmass. Superimposed are theoretical curves for ground-based instruments at various altitudes.  |  |
| COMPUTE_PARALLAXES*    | N   | <i>Boolean</i>                                     |
|                        | If true (Y), compute approximate parallaxes for all sources with at least three observations.<br>If false (N), this step is skipped.  |  |
| COMPUTE_PROPERMOTIONS* | N   | <i>Boolean</i>                                     |
|                        | If true (Y), compute proper motions for all sources with at least two observations. If false (N), this step is skipped.   |  |
| CORRECT_COLOURSHIFTS*  | N   | <i>Boolean</i>                                     |
|                        | If true (Y), try to compensate for the effects of Differential Chromatic Refraction (DCR) using source colour information extracted from multi-band photometry (when available) to compute individual proper motions. If false (N), this step is skipped. |  |
| CROSSID_RADIUS         | 2.0   | <i>float</i>                                       |
|                        | Search radius (in arcsec) used for all cross-identifications.   |  |
| DISTORT_KEYS           | XWIN_IMAGE, YWIN_IMAGE  | <i>strings</i> ( $n \leq 2$ )                      |
|                        | SExtractor measurements used to map astrometric distortions. Keywords preceded with a colon are interpreted as FITS image keywords instead of SExtractor parameters.  |  |
| DISTORT_GROUPS         | 1, 1  | <i>integers</i> ( $n = n_{\text{DISTORT\_KEYS}}$ ) |

Polynomial group which each distortion key belongs to.

|   |  |   |
|---|--|---|
| DISTORT_DEGREES   | 3  | <i>integers</i> ( $n = n_{\text{groups}}$ ) |
| Degree of each distortion polynomial group.   |  |   |
| ELLIPTICITY_MAX   | 0.5  | <i>float</i>                                |
| Maximum ellipticity (defined as $(r - 1)/(r + 1)$ , where r is the source aspect ratio $\geq 1$ ) allowed for input detections.                         |  |   |
| EXPOTIME_KEY  | EXPTIME  | <i>string</i>                               |
| FITS header keyword that stores the exposure time (in seconds). Exposure time is set to 1.0 if the keyword is not found.                                |  |   |
| EXTINCT_KEY   | PHOT_K   | <i>string</i>                               |
| FITS header keyword that stores the extinction coefficient (in magnitudes per unit air-mass). The extinction is set to 0.0 if the keyword is not found. |  |   |
| FGROUP_RADIUS   | 1.0  | <i>float</i>                                |
| Maximum angular distance (in degrees) allowed between field centres to include them in the same group of fields.  |  |   |
| FIXFOCALPLANE_NMIN*   | 1  | <i>integer</i>                              |
| Minimum number of detections per focal plane array required to be part of MOSAIC_TYPE FIX_FOCALPLANE statistics.  |  |   |
| FLAGS_MASK*   | 0x00fc   | <i>integer</i>                              |
| Binary mask applied to SExtractor's FLAGS parameters to reject flagged detections.  |  |   |
| FOCDISTORT_DEGREE*  | 1  | <i>integer</i>                              |
| Degree of the exposure-related focal plane distortion polynomial.   |  |   |
| FULLOUTCAT_NAME   | full.cat   | <i>string</i>                               |
| Filename of the output catalogue containing the full information about input detections. Used only if FULLOUTCAT_TYPE is different from NONE.           |  |   |
| FULLOUTCAT_TYPE   | NONE   | <i>keywords</i>                             |
| Format of the full output catalogue produced by SCAMP:  |  |   |
| NONE  | No output  |   |
| ASCII   | ASCII format   |   |
| ASCII_HEAD  | ASCII format preceded with comment lines listing column labels |   |
| ASCII_VOTABLE   | XML-VOTable format   |   |
| FITS  | Simple FITS binary table                                       |   |
| FITS_LDAC   | SExtractor binary catalogue format                             |   |

|  |  |  |
|--|--|--|
| FWHM_THRESHOLDS  | 0.0, 100.0   | <i>floats</i> ( $n = 2$ )                          |
| Range of Full-Width at Half-Maximum (as approximated by SExtractor's FLUX_RADIUS estimator) allowed for input detections.  |  |  |
| HEADER_SUFFIX  | .head  | <i>string</i>                                      |
| Filename extension of header files returned by SCAMP.  |  |  |
| HEADER_TYPE*   | NORMAL   | <i>keyword</i>                                     |
| Type of information returned by SCAMP in header files:   |  |  |
| NORMAL   | Complete WCS information                             |  |
| FOCAL_PLANE  | Partial WCS information for mapping the focal-plane. |  |
| IMAFLAGS_MASK*   | 0x0  | <i>integer</i>                                     |
| Binary mask applied to SExtractor's IMAFLAGS parameters to reject flagged detections.  |  |  |
| INCLUDE_ASTREFCATALOG*   | Y  | <i>Boolean</i>                                     |
| If true (Y), include observations from the astrometric reference catalogue to compute individual proper motions. If false (N), only detections from input catalogues are used.   |  |  |
| MAGZERO_INERR  | 0.01   | <i>floats</i> ( $n \leq n_{\text{phot\_instru}}$ ) |
| Typical magnitude <i>systematic</i> errors expected between overlapping photometric exposures before calibration.  |  |  |
| MAGZERO_KEY  | PHOT_C   | <i>string</i>                                      |
| FITS header keyword which stores the magnitude zero-point (in magnitudes "per second"). The zero-point is set to 0.0 if the keyword is not found.  |  |  |
| MAGZERO_OUT  | 0.0  | <i>floats</i> ( $n \leq n_{\text{phot\_instru}}$ ) |
| Arbitrary magnitude zero-point used by SCAMP for its output flux scale.  |  |  |
| MAGZERO_REFERR   | 0.03   | <i>floats</i> ( $n \leq n_{\text{phot\_instru}}$ ) |
| Typical magnitude <i>systematic</i> errors expected between overlapping non-photometric exposures after calibration.   |  |  |
| MATCH  | Y  | <i>Boolean</i>                                     |
| If true (Y), matching of input detections with sources from the astrometric reference catalogue is attempted, and exposures are registered (with accuracy defined by MATCH_RESOL). If false (N), this step is skipped. |  |  |
| MATCH_FLIPPED  | Y  | <i>Boolean</i>                                     |
| If true, a possible flipping of input frames is considered during matching. Should be $\leq$ CROSSID_RADIUS.   |  |  |
| MATCH_NMAX*  | 0  | <i>integer</i>                                     |

Maximum number of detections to use to compute the position angle and pixel scale in the pattern matching phase. 0 (default) for automatic.

MATCH\_RESOL 0.0 float

Resolution (in arcsec) at which matching is performed. 0 (default) for automatic.

MERGEDOUTCAT\_NAME scamp.cat string

Filename of the merged catalogue produced by SCAMP.

## Format of the merged catalogue produced by SCAMP:

NONE No output

ASCII                          ASCII format

**ASCII\_HEAD** ASCII format preceded with comment lines listing column labels

## ASCII\_VOTABLE      XML-VOTable format

## FITS Simple FITS binary table

## FITS\_LDAC SExtractor binary catalogue format

MOSAIC\_TYPE UNCHANGED *keywords* ( $n \leq n_{\text{astr\_instru}}$ )

Type of pre-processing for mosaics of focal plane arrays (multi-extension FITS catalogues):

UNCHANGED No pre-processing

**SAME\_CRVAL** Set all extensions to the same CRVAL $i$  WCS parameters, without compensating the shift by adjusting other parameters

**SHARE\_PROJAXIS** Bring all extensions to a common set of CRVAL $i$  WCS parameters and compensate by adjusting the CRPIX $i$  and CD $i,j$  parameters

**FIX\_FOCALPLANE** Attempt to derive a consistent placement of focal plane arrays by first applying the **SHARE\_PROJAXIS** procedure, and then computing the median position of detectors

**LOOSE** Treat focal plane arrays as mechanically unconnected devices; even pattern matching is performed independently for every extension

NTHREADS 0 *integer*

Number of threads (processes) to be used for parallel computations. If **NTHREADS** is 0, the number of threads is automatically set to the number of logical processor cores in the system. If **NTHREADS** if negative, SCAMP chooses the lowest between  $|NTHREADS|$  and the number of logical cores in the system.

PHOT\_ACCURACY\* 0.01 float

Additional photometric uncertainty parameter, added in quadrature to photometric uncertainties computed by SExtractor.

**PHOTCLIP\_NSIGMA\*** 3.0 *float*

Clipping threshold for the second photometric pass, in units of standard deviation.

**PHOTFLUX\_KEY** **FLUX\_AUTO** *string*  
SExtractor measurement used as a flux estimate in the input catalogues.

**PHOTFLUXERR\_KEY**                   **FLUXERR\_AUTO**                   *string*  
SExtractor measurement used as a flux error estimate in the input catalogues.

**PIXSCALE\_MAXERR** 1.2 *float*  
Search range of the pixel scale factor used in the astrometric MATCHing procedure. 1.2 (times) is equivalent to a range of  $\pm 20\%$  in pixel scale compared to what is stated in the WCS CD matrix of the original image headers.

| PROJECTION_TYPE                               | SAME   | <i>keywords</i> |
|---|--|-----------------|
| World Coordinate System projection in output: |  |                 |
| TPV   | Distorted tangential as described by the TPV FITS convention<br>(added officially to the FITS registry in Aug. 2012) |                 |
| TAN   | Distorted tangential (Greisen & Calabretta's 2000 draft, obsoleted)  |                 |
| SAME  | Same as input (distorted TAN or TPV)   |                 |

**REFOUT\_CATPATH** . *string*  
Directory path where reference catalogues will be saved (if **SAVE\_REFCATALOG** is set to Y).

**REF\_PORT\*** 80 *string*  
Port number to connect to the Vizier server for reference catalogues.

|  |  |   |
|--|--|---|
| <b>REF_SERVER</b>  | <b>cocat1.u-strasbg.fr</b>   | <i>string</i>                                 |
| IP address of the Vizier server for reference catalogues. The default is the CDS server in Strasbourg, France. Other possible servers include  |  |   |
| <b>axel.u-strasbg.fr</b>   | : CDS backup server in Strasbourg, France  |   |
| <b>vizier.hia.nrc.ca</b>   | : Vizier server at CADC, Victoria, Canada  |   |
| <br>   |  |   |
| <b>SAVE_REFCATALOG</b>   | <b>N</b>   | <i>Boolean</i>                                |
| If true, a copy of the reference catalogues downloaded from <b>REF_SERVER</b> will be saved in FITS_LDAC format to <b>REFOUT_CATPATH</b> .   |  |   |
| <br>   |  |   |
| <b>SN_THRESHOLDS</b>   | <b>10.0, 100.0</b>   | <i>floats (n = 2)</i>                         |
| The first number is the minimum signal-to-noise that a SExtractor detection should possess to be kept in SCAMP. The second number is the minimum signal-to-noise for a source to be part of the "high S/N" class in SCAMP plots and statistics. Signal-to-noise is defined in SCAMP as the ratio between flux and flux ( <i>rms</i> ) uncertainty. |  |   |
| <br>   |  |   |
| <b>SOLVE_ASTROM</b>  | <b>Y</b>   | <i>Boolean</i>                                |
| If true (Y), an astrometric solution is computed in 2 passes. If false (N), this step is skipped (but statistics about astrometry are still computed).   |  |   |
| <br>   |  |   |
| <b>SOLVE_PHOTOM</b>  | <b>Y</b>   | <i>Boolean</i>                                |
| If true (Y), a photometric solution is computed in 2 passes. If false (N), this step is skipped (but statistics about photometry are still computed).  |  |   |
| <br>   |  |   |
| <b>STABILITY_TYPE</b>  | <b>INSTRUMENT</b>  | <i>keywords (n ≤ n<sub>astr_instru</sub>)</i> |
| Tells SCAMP how to compute distortion patterns (§6.9.1), depending on the stability of the astrometric instruments:  |  |   |
| <b>INSTRUMENT</b>  | Stability extends over all the exposures of a given astrometric instrument; both common distortion pattern will be computed  |   |
| <b>PRE-DISTORTED</b>   | SCAMP assumes that a valid distortion pattern is encoded in the input headers and  |   |
| <b>EXPOSURE</b>  | The instrument is unstable from exposure to exposure, and a different distortion pattern has to be computed for each of them |   |
| <br>   |  |   |
| <b>VERBOSE_TYPE</b>  | <b>NORMAL</b>  | <i>keyword</i>                                |
| Degree of verbosity of the software on screen:   |  |   |
| <b>QUIET</b>   | No Output besides warnings and error messages  |   |
| <b>NORMAL</b>  | "Normal" display with messages updated in real time using ASCII escapes-sequences  |   |
| <b>LOG</b>   | Like NORMAL, but without real-time messages and ASCII escape-sequences   |   |
| <b>FULL</b>  | Everything   |   |
| <br>   |  |   |
| <b>WEIGHTFLAGS_MASK*</b>   | <b>0x00ff</b>  | <i>integer</i>                                |

Binary mask applied to SExtractor’s `FLAGS_WEIGHT` parameters to reject flagged detections.

`WRITE_XML` *Boolean*

If true (Y), an XML summary file will be written after completing the processing.

`XML_NAME` *string*

File name for the XML output of SCAMP.

`XSL_URL*` *string*

URL of an XSL style-sheet for the XML output of SCAMP. This URL will appear in the `href` attribute of the `style-sheet` tag.

## 6 How SCAMP works

### 6.1 Overview of the software

What SCAMP does is basically to read a set of input catalogues and their preliminary, approximate astrometric data, compute a proper astrometric and photometric solution, and finally save the result of this calibration in header files. The work can be decomposed into several steps:

1. Input catalogues and headers are read and checked for content. SCAMP sorts catalogues by position on the sky (“groups of fields”) as well as astrometric and photometric contexts (“instruments”).
2. Mosaics of detectors undergo a specific pre-treatment to homogenise the astrometric calibration across the focal plane.
3. A catalogue of astrometric standards (“reference catalogue”) is downloaded from the Vizier database for every group.
4. The reference catalogues are utilised by a pattern matching procedure to register all input catalogues.
5. All detections and reference sources are cross-matched and an astrometric solution is computed. This operation is repeated after clipping of outliers.
6. A photometric solution is computed in two passes (and outliers are clipped at each iteration).
7. Updated astrometric and photometric calibration data are written to external headers.

The global layout of SCAMP is presented in Fig. 1. Let us now describe each of the important steps.

### 6.2 Parallel processing

SCAMP is largely multithreaded, which means it will take advantage of multiple processors/cores in the machine it is run on for its most CPU-intensive tasks. The maximum number

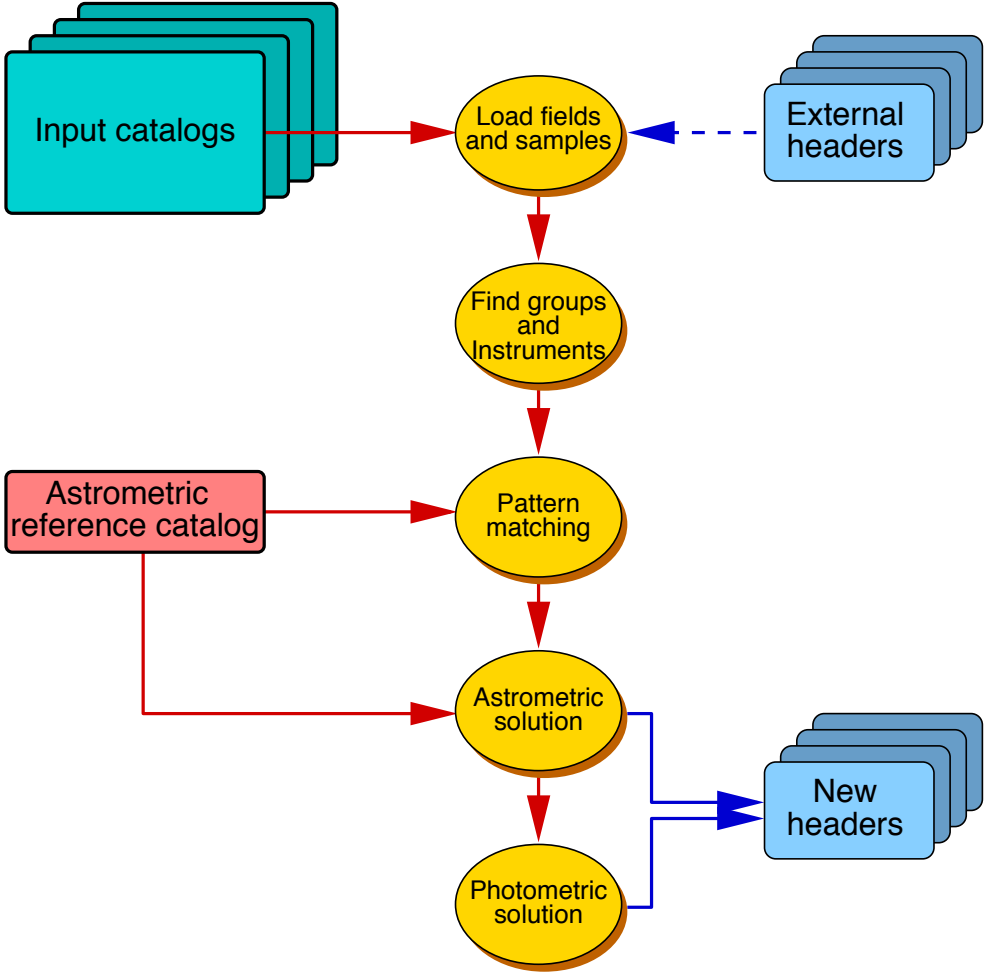


Figure 1: Global Layout of SCAMP.

of active threads (processes) is set by the `NTHREADS` configuration parameter. Best performance is generally achieved with `NTHREADS` equal to the number of available processor cores. On a Linux or similar POSIX-compliant system, SCAMP will automatically use as many threads as there are processors/cores in the machine if `NTHREADS` is 0 (the default). Figure 2 shows the improvement in SCAMP processing speed as a function of `NTHREADS` on an 8-core machine. Departure from a linear scaling with the number of threads is presently due to segments of code that not yet multithreaded. As Fig. 2 shows, performance decreases as the number of threads exceeds the number of physical cores/processors. Note that the actual processing time and the speed-up gained by parallelisation are not simple functions of the number of detections, but are in addition closely related to the exposure dithering pattern.

## 6.3 Loading data

### 6.3.1 Preparing good input catalogues

The accuracy of the calibrations performed by SCAMP depend, among other things, on the quality of the catalogues provided in input. Here are a few rules to prepare good catalogues with SExtractor:

- For images taken with electronic cameras, use as positional measurements the `WIN` pa-

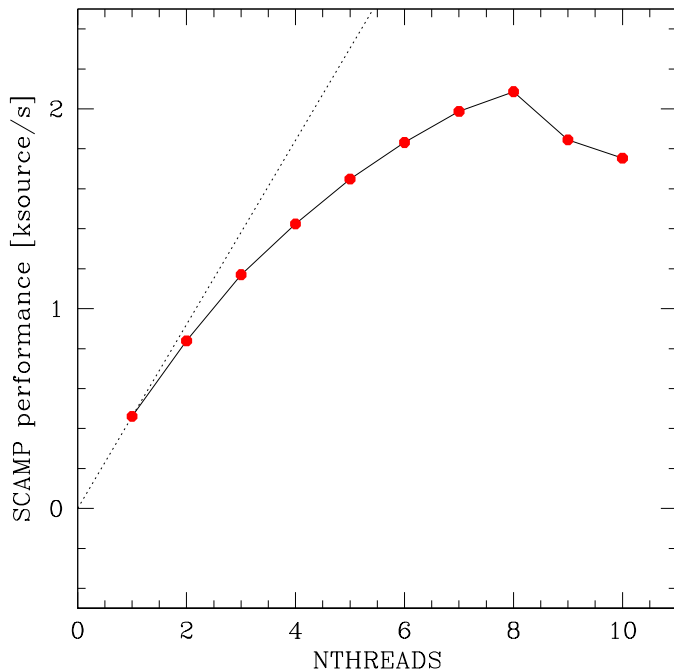


Figure 2: Processing speed of SCAMP, in thousands of sources per second, 1.2.11 for the full astrometric+photometric calibration for 144 CFHT-MEGACAM overlapping fields ( $\approx 4.10^6$  detections), as a function of the `NTHREADS` configuration parameter, on an SMP machine with four Opteron-875 2.2GHz dual-core processors (8 cores). Optimum performance is obtained when the number of threads equals the number of processor cores. Perfect linear scaling is indicated by the dashed line for reference.

rameters from the latest versions of SExtractor . They are about three times less noisy than the old isophotal measurements for high signal-to-noise objects. For photographic plates, the standard `X_IMAGE`, `Y_IMAGE` are more reliable.

- Make sure that the extraction `FLUX_RADIUS` and `FLAGS` are present in the catalogues, and that the `GAIN` and `SATUR_LEVEL` configuration parameters in `SEXTRACTOR` are set to proper values. These allow SCAMP to filter out saturated sources and provide correct weights to detections.
- Use weight-maps and include the `FLAGS_WEIGHT` measurement parameter if frames include overscans, bad columns and other unreliable image areas, or if noise is unevenly distributed. Not only this will allow SCAMP to discard artifacts and detections truncated by defects, but it will also help `SEXTRACTOR` compute a more reliable background map, free of spurious gradients that may corrupt centroid measurements.
- Use flag-maps and the `IMAFLAGS_ISO` measurement parameter in `SEXTRACTOR` to identify sources you might later want to turn “off” or “on” for calibration using SCAMP’s `IMAFLAGS_MASK` configuration option.
- Unless the number of detections per FITS image (or FITS extension) is dangerously low

(less than a few tens), it is generally counterproductive to apply a very low detection threshold, as it would activate the deblending of otherwise isolated objects.

- Be very careful of `.head` header files produced by a previous SCAMP run that may inadvertently be read by some versions of SExtractor while (re-)doing the source extraction, and override WCS parameters from the original image headers in subsequent SCAMP calls.

### 6.3.2 Filtering detections

Corrupted detections degrade the quality of calibrations, and must be filtered out when reading the catalogues. SCAMP directly rejects:

- detections for which the signal-to-noise (defined as the ratio between flux and flux *rms* uncertainty) is less than the first argument of the `SN_THRESHOLDS` configuration parameter. In practice, sources with signal-to-noise ratios below 10 (the default), are generally not worth including unless they appear in exceedingly large proportions.
- detections with Full-Widths at Half-Maximum beyond the range set by the `FWHM_THRESHOLDS` configuration parameter (in pixels). The default range is 0,100. Use more restrictive values to filter out small glitches like cosmic ray hits and/or large image artifacts like optical ghosts. `FLUX_RADIUS` measurements must be present in the input catalogues for the filtering to work.
- detections with flags that match SCAMP rejection masks. The `FLAGS_MASK` “advanced” configuration parameter defines the binary mask associated to SExtractor’s extraction `FLAGS`. Its default value is the hexadecimal value `00fc`, which means that all “true” flag bits but bit 0 (crowded region) and bit 1 (deblended object) trigger a rejection of the parent detection. Setting `FLAGS_MASK` to `00ff` would also remove from the set of accepted detections those flagged as deblended and those flagged as crowded, which can be useful whenever only perfectly isolated sources must enter the solution. “Advanced” configuration parameters `IMAFLAGS_MASK` and `WEIGHTFLAGS_MASK` work as `FLAGS_MASK`; they operate respectively on SExtractor’s `IMAFLAGS_ISO` and `FLAGS_WEIGHT`<sup>9</sup> flags.
- detections with abnormal measurements (such as positional uncertainties equal to zero or positions outside frame boundaries), caused by software bugs or image artifacts.

## 6.4 Sorting the catalogues

SCAMP automatically sorts input catalogues according to three partitioning schemes: field groups, astrometric instruments, and photometric instruments. These three schemes define to a large extent how degrees of freedom are distributed during calibration.

### 6.4.1 Field groups

In SCAMP, a field group is an ensemble of overlapping exposures (“fields”, represented by catalogue files) in a given part of the sky: field groups are assembled on the basis of the relative positioning of fields. The current algorithm to assign a group to an exposure is still crude: a field is said to belong to the same group as another field if the angular distance between their

---

<sup>9</sup>`FLAGS_WEIGHT` will be available in SExtractor starting from version 2.4.5.

centres is less than  $r_g$ . The value of  $r_g$  is set using the `FGROUP_RADIUS` configuration parameter (in degrees). It must include all pointing uncertainties. The default value is 1 degree: it is appropriate for wide-field instruments, but you might want to decrease it if your observations consist of a number of close, albeit non-overlapping “clusters” of narrow-field exposures.

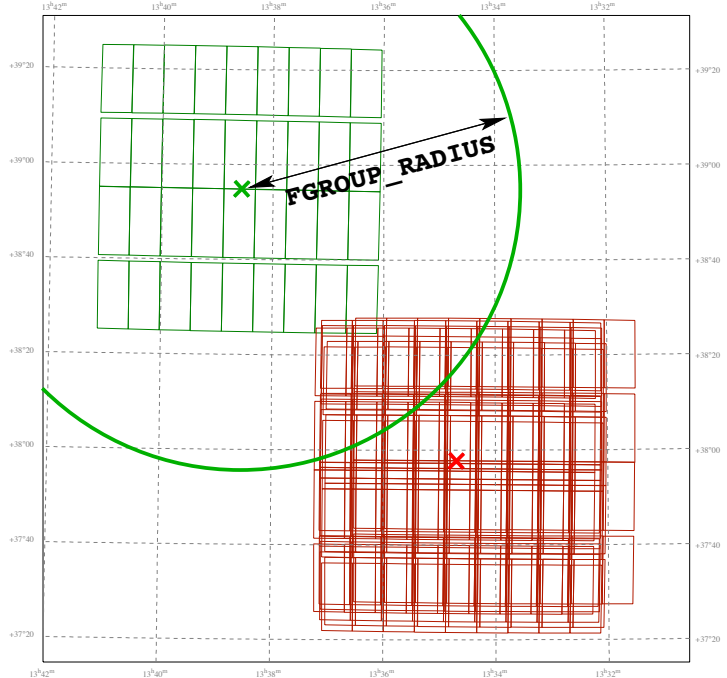


Figure 3: In this example with 8 CFHT-MEGACAM catalogues (36 CCDs each), one of the exposures (green) will not be associated with the (red) group on the lower right of the plot because the distance between its centre (green cross) and the nearest one (centre marked with a red cross) exceeds the distance specified by `FGROUP_RADIUS`. As a result, a second group containing a single catalogue will be created.

#### 6.4.2 Astrometric instruments

To derive an accurate astrometric solution, it is important to isolate contexts within which the instrument behaves in a predictable way. This brings us to the concept of “astrometric instrument”: in SCAMP two different “astrometric instruments” may represent either two physically distinct devices like two different cameras, or the same device operating in two different conditions from the point of view of non-linear astrometric distortions. For instance, in many cases the same camera operating with three different filters will exhibit three slightly different distortion patterns: these three contexts of observing must be considered as 3 different astrometric instruments. A camera might be dismounted from the telescope or mechanically adjusted between two sets of exposures: it is then *a priori* safer to consider that this leads to two different astrometric instruments. Note that a purely linear change of the distortion pattern such as a shift, a rotation, a rescaling, a shear and/or a flattening has no influence since these are all considered as free parameters for each exposure.

SCAMP identifies astrometric instruments according to the contents of a set of FITS keywords. These FITS keywords must be given as arguments to the `ASTRINSTRU_KEY` configuration parameter. They main contain integers, decimal numbers, character strings or even Booleans; to each distinct combination of contents of these FITS keywords will be associated a different

astrometric instrument. The default for `ASTRINSTRU_KEY` is the pair `FILTER,QRUNID`; although the first argument is widely used and self-explaining, the second one is quite specific to the Canada-France-Hawaii Telescope (it identifies the observing run), and therefore one might want to change it if working with images from other observatories. As one might guess, identifying the right astrometric contexts requires some knowledge of the instrument and the history of observations: how stable with time are the optical system and the focal plane? Is a field rotator involved? Was the instrument touched during the day? When in doubt, especially in case of unexpectedly large residuals in the astrometric calibration, one may re-run SCAMP with `STABILITY_TYPE EXPOSURE` to check whether this improves the solution or not (this option treats each exposure as a different astrometric instrument, see §6.9.1).

#### 6.4.3 Photometric instruments

Photometric instruments are to photometry what astrometric instruments are to astrometry. However, photometric instruments are generally less sensitive than astrometric ones, since there are no mechanical effects involved here. Moreover the handling of photometry is still simplistic in the current version of SCAMP, and colour term variations are ignored. The only free parameter from exposure to exposure is the magnitude zero-point.

The `PHOTINSTRU_KEY` configuration parameter is set by default to `FILTER`. Be careful: this keyword is used at many different observatories but its contents does not follow strict naming conventions, and generally ignores all other contributions to the global spectral response. For instance, the “U” filter on some instrument may differ significantly from the “U” filter quoted in images from another instrument.

### 6.5 Pre-processing of mosaics

SCAMP can handle catalogues from both simple imaging devices and mosaics of detectors (“Focal Plane Arrays”, or FPAs). For the latter, catalogues are assumed to be in Multi-Extension FITS (MEF) format. SExtractor automatically creates MEF catalogues from MEF images. SCAMP can manipulate mosaics in a number of ways to perform the matching of sources on the sky, and the astrometric calibration itself. The user can control the policy of SCAMP regarding mosaics of every astrometric instrument with the `MOSAIC_TYPE` configuration parameter:

- In the `UNCHANGED` mode, the relative positioning of detectors on the focal plane, as recorded in the WCS keywords of the FITS headers, is assumed to be correct and constant from exposure to exposure. Matching with the reference catalogue will be done for all the detectors at once. This is the default.
- In the `SHARE_PROJAXIS` mode, the relative positioning of detectors is assumed to be constant and correct, but the different extensions within the same catalogue file do not share the same projection axis (the `CRVAL` FITS WCS keywords are different): although this does not prevent SCAMP from deriving an accurate solution, this is generally not an efficient astrometric description of the focal plane. This option brings all extensions to the same centered projection axis while compensating with other WCS parameters.
- `SAME_CRVAL`, like `SHARE_PROJAXIS` above, brings all extensions to the same centered projection axis (`CRVAL` parameters), but does not compensate by changing other WCS parameters. This option is useful when the `CRPIX` and `CD` WCS parameters are overrided by some focal plane model stored in a global `.ahead` file.

- The `FIX_FOCALPLANE` mode applies first a `SHARE_PROJAXIS` correction to the headers and then attempts to derive a common, “median” relative positioning of detectors within the focal plane. This mode is useful to “fix” the positions of detectors when these have been derived independently at each exposure in an earlier not-so-robust calibration (Fig. 4). A minimum of 5 exposures per astrometric instrument is recommended.
- Finally, the `LOOSE` mode makes all detector positions to be considered as independent between exposures. Contrary to other modes, matching with the reference catalogue will be conducted separately for each extension. The `LOOSE` mode is generally used for totally uncalibrated mosaics in a first SCAMP pass before doing a `FIX_FOCALPLANE`.

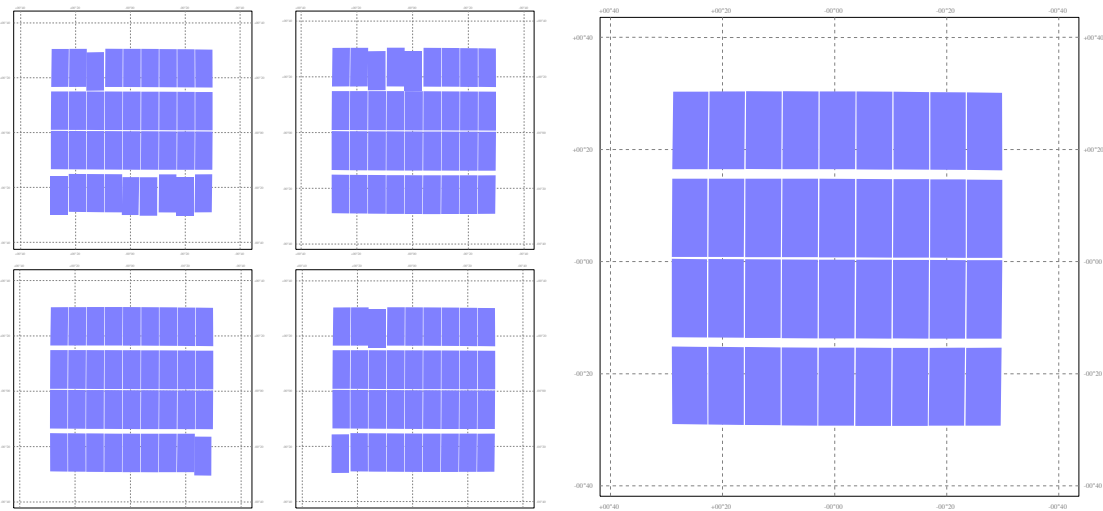


Figure 4: Result of `MOSAIC_TYPE FIX_FOCALPLANE` applied to 7 catalogues extracted from 7 MEF CFHT-MEGACAM images (mosaic of 36 CCDs/extensions). *Left:* relative positions of CCDs on the sky as described in the original FITS headers, for 4 of the 7 exposures. It appears that the centering procedure done at the telescope has failed on some CCDs. *Right:* “median” model recovered by SCAMP from the 7 exposures, with the `MOSAIC_TYPE FIX_FOCALPLANE` option.

## 6.6 Astrometric reference catalogues

Astrometric reference catalogues are required in SCAMP to locate precisely the exposures on the celestial sphere, and to attach the solution to a standard, well calibrated system. The `ASTREF_CATALOG` configuration parameter tells SCAMP how the reference catalogue(s) should be retrieved. A reference catalogue can either be loaded from a collection of local files (`ASTREF_CATALOG FILE`), or directly downloaded from a Vizier server (Ochsenbein et al., 2000), using one of the codes in Table 1. In both cases, SCAMP will only pick sources within a certain radius around each group<sup>10</sup> (§6.4.1). This radius is computed by SCAMP; it includes the positional uncertainties associated to the original images (§6.7).

The astrometric reference catalogues available in SCAMP are queried from Vizier through the `CDSCLIENT` package<sup>11</sup>, is given in Table 1. The `CDSCLIENT` must have been installed before running SCAMP. The path to the executable run by SCAMP is set by the `CDSCLIENT_EXEC`

<sup>10</sup>This simple procedure can be quite inefficient for observations carried along narrow strips. It is a limitation of the current versions of SCAMP.

<sup>11</sup><http://cdsweb.u-strasbg.fr/doc/cdsclient.html>. Make sure you have the latest version.

configuration parameter; the default is `/usr/local/bin/aclient.cgi`. The Vizier server IP address and port can be specified in SCAMP using the `REF_SERVER` and `REF_PORT` configuration parameters. The main CDS server in Strasbourg, France is used by default. Depending on where your machine is located, you might want to try other servers to achieve faster downloads (see p.16 for a list of alternative servers). Since SCAMP V1.7 the default `REF_PORT` is 80, which also tells CDSclient to use HTTP as a communication protocol. Using the HTTP instead of the original CDSclient protocol (port 1660) makes it possible for machines sitting behind a firewall and a proxy server to access reference catalogue data. All it takes is to set from your shell the `http_proxy` environment variable before running SCAMP using `export http_proxy=http://your_proxy` (from `sh` or `bash`) or `setenv http_proxy=http://your_proxy` (from `csh` or `tcsh`).

The default catalogue `ASTREF_CATALOG` is `USNO-B1`. It is not the best in terms of astrometric accuracy. It is however still currently the densest all-sky catalogue available, and is generally the most appropriate for calibrating deep-sky optical images at high-galactic latitude. Alternatively, `GSC-2.3` often does a better job, especially in regions of high stellar densities. `2MASS` is an infrared catalogue particularly appropriate for all observations conducted at wavelengths past 1 micron; it also generally fares better than `USNO-B1` with most optical images. If, by chance, your observations fall in the 35% of the sky covered by the `SDSS-R9`, you should definitely use the latter. `PPMX` and `UCAC-4` are the preferred catalogues for shallow exposures (brighter than 16th mag), whereas `TYCHO-2` should be reserved for the smallest telescopes and cameras+objectives with a field of view  $\geq 10$  sq.deg.

The matching and fitting procedures described next exhibit some dependency on magnitudes from the reference catalogue. As most reference catalogues are multiband, choosing one band instead of another may improve or degrade the results, depending on the affinity with the observation passbands. For instance, a less sensitive “red” channel may yield a larger number of bright reference sources than a more sensitive but “bluer” channel in a sky region with strong interstellar reddening; such reddened sources would help matching observations made in the red or near-infrared but would bring confusion for matching observations made with a “blue” filter.

The default behaviour of SCAMP is to use a pre-selected passband for each remote reference catalogue. The name of this passband is displayed at runtime and written in the XML output file. The reference passband can be changed with the `ASTREF_BAND` configuration parameter, either by giving explicitly the name of the chosen filter (see Table 1), or by indicating `BLUEST` or `REDDEST` to select the passband with the shortest or longest effective wavelength, respectively.

The acceptable magnitude range in the selected passband can be restricted on the bright end or the faint end (or both) using the `ASTREFMAG_LIMITS` configuration parameter; this is particularly convenient when calibrating shallow exposures on very wide fields of view.

## 6.7 Matching with the reference catalogues

Before proceeding further, SCAMP must locate every exposure on the sky with the help of the reference catalogue(s): this is the matching procedure. Matching is a time-consuming operation, and if by chance all images are already registered with sufficient accuracy — that is, better than `CROSSID_RADIUS`, see p.29 —, one should consider skipping this step by setting the `MATCH` configuration parameter to `N` (default is `Y`).

First, four parameters are derived during the matching procedure. These parameters are corrections to the initial WCS parameters present in the original image headers and/or in the related `.ahead` files: the relative pixel scale, the relative position angle, and the shifts in right ascension

Table 1: List of supported astrometric reference catalogues

| Code    | Real name   | Coverage                               | Density <sup>a</sup> | Bands                       | Mag. limit         | $\sigma_{\text{pos.}}^b$ | System <sup>c</sup> | Epochs <sup>d</sup> | Proper motions |
|---------|---|--|----------------------|-----------------------------|--------------------|--------------------------|---------------------|---------------------|----------------|
| GSC-1.3 | Guide-Star Catalog ACT V1.3 <sup>e</sup>                          | All sky                                | 610                  | V                           | $V \approx 15.5$   | 0.3"                     | FK5                 | 1975-1988           |                |
| GSC-2.2 | Guide-Star Catalog ACT V2.2.1 <sup>f</sup>                        | All sky                                | 11050                | $B_J, V, R_F, I_N$          | $B_J = 19.5$       | 0.3"                     | ICRS                | 1975-2000           |                |
| GSC-2.3 | Guide-Star Catalog ACT V2.3.2 <sup>g</sup>                        | All sky                                | 22920                | $U, B, B_J, V, R_F, I_N$    | $B_I = 21.5$       | 0.3"                     | ICRS                | 1975-2000           | ✓              |
| USNO-A1 | PMM US Naval Observatory A1.0 <sup>h</sup>                        | All sky                                | 11830                | $B_J, R_F$                  | $B_J \approx 19.5$ | 0.3"                     | FK5                 | 1949-1990           |                |
| USNO-A2 | PMM US Naval Observatory A2.0 <sup>i</sup>                        | All sky                                | 12760                | $B_J, R_F$                  | $B_J \approx 19.5$ | 0.3"                     | ICRS                | 1949-1990           |                |
| USNO-B1 | US Naval Observatory B1.0 <sup>j</sup>                            | All sky                                | 25350                | $B_J, R_F, I_N$             | $B_J \approx 21$   | 0.3"                     | ICRS                | 1949-2002           | ✓              |
| TYCHO-2 | Tycho-2 Catalogue of the 2.5 Million Brightest Stars <sup>k</sup> | All sky                                | 60                   | $B_T, V_T$                  | $V_T \approx 11$   | 6-60 mas                 | ICRS                | 1991                |                |
| UCAC-1  | 1st USNO CCD Astrograph Catalog <sup>l</sup>                      | $\delta \leq -15^\circ$                | ≈ 1500               | $R_U$                       | $R_U = 16$         | 70 mas                   | ICRS                | 1998-1999           | ✓              |
| UCAC-2  | 2nd USNO CCD Astrograph Catalog <sup>m</sup>                      | $\delta \leq +40^\circ$                | ≈ 1500               | $R_U$                       | $R_U = 16$         | 70 mas                   | ICRS                | 1998-2002           | ✓              |
| UCAC-3  | 3rd USNO CCD Astrograph Catalog <sup>n</sup>                      | All sky                                | 2440                 | $R_U$                       | $R_U \approx 16.3$ | 70 mas                   | ICRS                | 1998-2004           | ✓              |
| UCAC-4  | 4th USNO CCD Astrograph Catalog <sup>o</sup>                      | All sky                                | 2760                 | $R_U$                       | $R_U \approx 16.3$ | 70 mas                   | ICRS                | 1998-2004           | ✓              |
| NOMAD-1 | Naval Obs. Merged Astrom. Dataset <sup>p</sup>                    | All sky                                | 27090                | $B, V, R, J, H, K_s$        | $B \approx 21$     | 0.3"                     | ICRS                | 1949-2002           | ✓              |
| PPMX    | Position and Proper Motions eXtended <sup>q</sup>                 | All sky                                | 440                  | $B, V, R_U, R_F, J, H, K_s$ | $R_f \approx 15.2$ | 40 mas                   | ICRS                | 1975-2002           | ✓              |
| CMC-14  | Carlsberg Meridian Catalog number 14 <sup>r</sup>                 | $-30^\circ \leq \delta \leq +50^\circ$ | 3700                 | $r, J, H, K_s$              | $r \approx 17$     | 90 mas                   | ICRS                | 1999-2005           |                |
| 2MASS   | 2-Micron All Sky Survey point source <sup>s</sup>                 | All sky                                | 11420                | $J, H, K_s$                 | $J = 17.1$         | 0.15"                    | ICRS                | 1997-2000           |                |
| DENTS-3 | DEep Near Infrared Survey version 3 <sup>t</sup>                  | $\delta < +2^\circ$                    | 21270                | $i, J, K_s$                 | $i \approx 18.5$   | 0.2"                     | ICRS                | 1996-2001           |                |
| SDSS-R3 | Sloan Digital Sky Survey release 3 <sup>u</sup>                   | 5282 deg <sup>2</sup>                  | 27660                | $u, g, r, i, z$             | $r = 22.2$         | 80 mas                   | ICRS                | 2000-2003           |                |
| SDSS-R5 | Sloan Digital Sky Survey release 5 <sup>v</sup>                   | 8000 deg <sup>2</sup>                  | 26880                | $u, g, r, i, z$             | $r = 22.2$         | 50 mas                   | ICRS                | 2000-2005           |                |
| SDSS-R6 | Sloan Digital Sky Survey release 6 <sup>w</sup>                   | 9580 deg <sup>2</sup>                  | 29950                | $u, g, r, i, z$             | $r = 22.2$         | 50 mas                   | ICRS                | 2000-2006           |                |
| SDSS-R7 | Sloan Digital Sky Survey release 7 <sup>x</sup>                   | 11660 deg <sup>2</sup>                 | 30610                | $u, g, r, i, z$             | $r = 22.2$         | 50 mas                   | ICRS                | 2000-2008           |                |
| SDSS-R8 | Sloan Digital Sky Survey release 8 <sup>y</sup>                   | 14555 deg <sup>2</sup>                 | 32230                | $u, g, r, i, z$             | $r = 22.2$         | 50 mas                   | ICRS                | 2000-2010           |                |
| SDSS-R9 | Sloan Digital Sky Survey release 9 <sup>z</sup>                   | 14555 deg <sup>2</sup>                 | 32230                | $u, g, r, i, z$             | $r = 22.2$         | 50 mas                   | ICRS                | 2000-2010           |                |

<sup>a</sup>Mean density in deg<sup>-2</sup>; all-sky surveys have a strongly skewed density distribution, and therefore their density at high galactic latitudes is significantly lower.

<sup>b</sup>Typical 1-dimensional scatter rms observed in comparisons with accurate CCD measurements. This does not include systematics on large scales, which can be up to 1° in some survey areas.

<sup>c</sup>Celestial coordinate reference system for source positions.

<sup>d</sup>Main range of observation epochs for source positions. Source positions are reconstructed to epoch J2000.0 in the USNO-B1, Tycho-2, UCAC-2/3/4, and PPMX catalogues.

<sup>e</sup>Lasker et al. (1990), Russell et al. (1990), Jenkner et al. (1990), Morrison et al. (2001)

<sup>f</sup><http://gss.strsci.edu/catalogs/GSC/GSC2/GSC2.htm>

<sup>g</sup>Lasker et al. (2008), <http://gss.strsci.edu/Catalogs/GSC/GSC2/GSC2.htm>

<sup>h</sup>Monet et al. (1998), <http://www.nofs.navy.mil/projects/pmm/readme.htm>

<sup>i</sup>Monet (1998), <http://www.nofs.navy.mil/projects/pmm/USNOA2doc.htm>

<sup>j</sup>Monet et al. (2003), <http://www.nofs.navy.mil/data/fchpix>

<sup>k</sup>Høg et al. (2000), <http://www.astro.ku.dk/~rik/Tycho-2>

<sup>l</sup>Zacharias et al. (2000), <http://www.usno.navy.mil/USNO/astrometry/optical-IR-prod/ucac>

<sup>m</sup>Zacharias et al. (2004b), <http://www.usno.navy.mil/USNO/astrometry/optical-IR-prod/ucac>

<sup>n</sup>Zacharias et al. (2010), <http://www.usno.navy.mil/USNO/astrometry/optical-IR-prod/ucac>

<sup>o</sup>Zacharias et al. (2012), <http://www.usno.navy.mil/USNO/astrometry/optical-IR-prod/ucac>

<sup>p</sup>Zacharias et al. (2004a), <http://www.nofs.navy.mil/nomad>

<sup>q</sup>Röser et al. (2008)

<sup>r</sup>Copenhagen University et al. (2006)

<sup>s</sup>Curri et al. (2003), <http://www.ipac.caltech.edu/2mass/>

<sup>t</sup>DENIS Consortium (2005), <http://cdsweb.u-strasbg.fr/denis.html>

<sup>u</sup>Abazajian et al. (2005), <http://www.sds.org/dr3/>

<sup>v</sup>Adelman-McCarthy et al. (2007), <http://www.sds.org/dr5/>

<sup>w</sup>Adelman-McCarthy et al. (2008), <http://www.sds.org/dr6/>

<sup>x</sup>Abazajian et al. (2009), <http://www.sds.org/dr7/>

<sup>y</sup>Aihara et al. (2011), <http://www.sdss3.org/dr8/>. Note that the new reductions used for the SDSS-DR8 have introduced some errors in the astrometry, especially at declinations  $\delta \geq 41$  deg; it is recommended to use SDSS-R9 instead whenever possible.

<sup>z</sup>Ahn et al. (2012), <http://www.sdss.org/dr8/>. Note that the new reductions used for the SDSS-DR8 have introduced some errors in the astrometry, especially at declinations  $\delta \geq 41$  deg; it is recommended to use SDSS-R7 instead whenever possible.

and declination. All the computations are performed in planar pixel coordinates (i.e. these are the astrometric references which are projected onto the focal plane, and not the detections which are de-projected onto the celestial sphere).

### 6.7.1 Finding the pixel scale and the position angle

Corrections to pixel scale and position angle are computed first. SCAMP basically uses the technique described by Kaiser et al. (1999): histograms of source pairs in  $\log(\text{distance})$  *vs* position-angle space are calculated for the reference catalogue and for the catalog to be matched (Fig.5). Both histograms are then cross-correlated and bandpass-filtered using Fast Fourier Transforms. A peak finder algorithm locates the correlation-peak, whose coordinates correspond to the relative position-angle and  $\log(\text{scalefactor})$  between the two catalogues. A “contrast” factor is computed in order to assess the reliability of the correlation: it is defined as the ratio of the amplitude of the detected peak (within the allowed limits in pixel scale and position angle) to the amplitude of the second highest peak found in the cross-correlation. In practice, contrast factors above  $\approx 2.0$  shall be considered as reliable, while contrasts below 2.0 are dubious.

Before proceeding to the next step, pixel scale and position angle are further refined by an iterative Gaussian centring of the correlation peak.

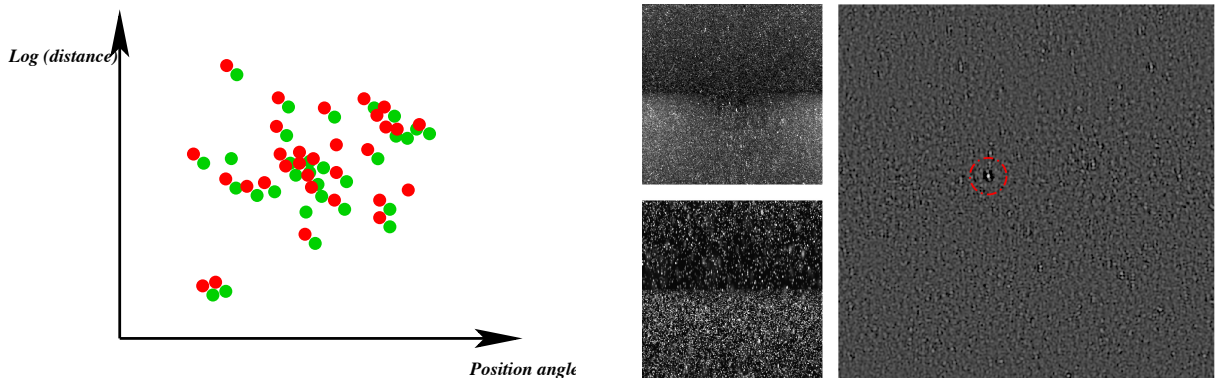


Figure 5: Computing the pixel scale and position angle corrections. *Left*: pixel scale and image orientation are found by measuring the shift between the 2D histograms of source pair coordinates in the  $\log(\text{projected distance})$  - position-angle space for input detections (green) and the reference catalogue (red). *Centre*: 2D histograms displayed in grey levels for one of the input catalogues (top), and the reference catalogue (bottom). Note that fluxes and uncertainties of source coordinates are taken into account, as can be seen in the larger (Gaussian) spread for pair vectors in the reference catalogue. *Right*: bandpass-filtered cross-correlation of the two histograms; the position of the correlation peak (marked with the red circle) gives the difference in orientation angle and  $\log(\text{scale})$  between both catalogues.

The recovery of true pixel scale and position angle corrections is controlled with the MATCH\_NMAX, MATCH\_RESOL, PIXSCALE\_MAXERR and POSANGLE\_MAXERR configuration parameters.

**MATCH\_RESOL** sets the resolution of the 2D histograms (in arcsec per pixel). The default value is 0, a special code that tells SCAMP to compute automatically the best matching resolution  $R$  for each frame. The procedure is the following. A first estimate of  $R$  is computed with

$$R = \sqrt{f_c \min(\rho, \rho_{\text{ref}})}, \quad (2)$$

where  $\rho$  and  $\rho_{\text{ref}}$  are respectively the average angular densities of sources in the catalogue to be matched and in the astrometric reference catalogue;  $f_c$  is a “confusion factor”  $<< 1$  : the average number of sources found in a small patch of angular area  $R \times R$  within the frame. It was found that a  $f_c$  of  $\approx 0.01$  (hardwired in SCAMP) gives the most reliable results in empty to moderately dense fields. In very crowded fields, it is necessary to impose a lower bound to the matching resolution as  $R$  can get smaller than the typical positional uncertainties. The lower bound  $R_{\min}$  is derived by taking the square-root of an average source “cross-section”. This cross-section is defined as the average area of the disk where a source has a probability  $1 - f_c$  to be found. Assuming a Gaussian distribution of source positions around their true locations (with variance  $\sigma^2$  or  $\sigma_{\text{ref}}^2$ ), one finds:

$$R_{\min} = \sqrt{-2\pi \max(\sigma^2, \sigma_{\text{ref}}^2) \ln f_c}. \quad (3)$$

The automatically derived value of the matching resolution should be appropriate for most wide-field images. One may however benefit from a manually entered value in cases where the reliability of detections is exceptionally poor.

**MATCH\_NMAX** is the maximum number of *unsaturated* sources that should be used for searching the pixel scale and position angle. This first part of the MATCHing procedure must examine each pair of detections; it can therefore become exceedingly slow in fields which contain a large number of sources. Suggested values of **MATCH\_NMAX** range from 1000 to 10000. With current computers, no more than 20,000 sources can be processed in a reasonable amount of time. In practice, we strongly recommend to leave **MATCH\_NMAX** to its default value 0, which triggers the following behaviour: MATCHing is first attempted with 2000 sources, and then increased by a factor of 2 until the contrast reaches 2.0 or more. The algorithm currently stops at 8000.

**PIXSCALE\_MAXERR** sets the search range for the scaling factor. The default is 1.2, which means a search range of  $\pm 20\%$  with respect to the pixel scale quoted in the original WCS header. In practice, search ranges up to 2 can be requested.

**POSANGLE\_MAXERR** sets the search range for the image orientation (position angle, in degrees) with respect to the one quoted in the original WCS header. The default value is 5 degrees, which means a search range of  $\pm 5^\circ$ . Values up to  $180^\circ$  (that is, the full circle) can be requested, but note that **POSANGLE\_MAXERRs**  $\geq 90^\circ$  require more processing time, because of the degeneracy between  $\theta$  and  $\theta + \pi$  for the orientation of pairs.

### 6.7.2 Finding the coordinate shift

Once the pixel scale and the position angle have been corrected, the shift in right ascension and declination between the catalogue to be matched and the reference catalogue is computed by simply cross-correlating the 2D histograms of projected source positions in both catalogues (Fig. 6). The **MATCH\_RESOL** configuration parameters play the same role as in §6.7.1. The search range (in arcminutes) is set with **POSITION\_MAXERR**. The default is  $1'$ .

### 6.7.3 Image flipping

SCAMP will check for a possible image flipping, at the expense of additional computations, if the **MATCH\_FLIPPED** configuration parameter is set to Y (default is N).

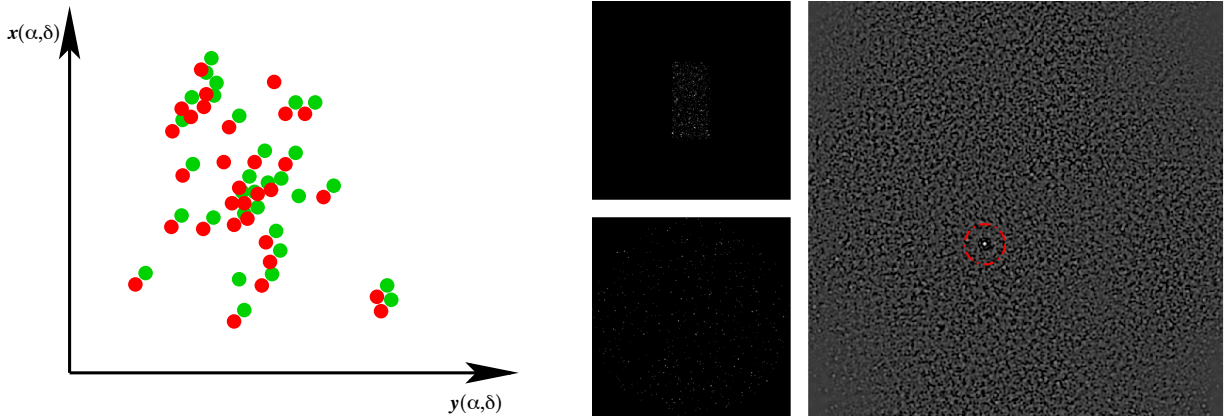


Figure 6: Computing coordinate shift. *Left*: The shift is measured between the 2D histograms of projected source coordinates  $x(\alpha, \delta)$  and  $y(\alpha, \delta)$  for input detections (green) and the reference catalogue (red). *Centre*: 2D histograms displayed in grey levels for one of the input catalogues (top), and the reference catalogue (bottom). *Right*: bandpass-filtered cross-correlation of the two histograms; the position of the correlation peak (marked with the red circle) gives the difference in position between both catalogues.

#### 6.7.4 Refining the matching procedure

Finally, a 2D regression is performed on the coordinates of detections matched with sources of the reference catalogue. This provides accurate parameters for a linear mapping of each exposure between the original ( $\xi$ ) and the final  $\xi'$  coordinates in the projected sky. The linear mapping is expressed as a combination of scale, rotation, shear and shift corrections:

$$\xi' = \mathbf{A}\xi + \Delta\xi \quad (4)$$

with

$$\mathbf{A} = \rho \begin{pmatrix} 1 + \frac{\gamma}{2}(1 + \cos 2\theta_\gamma) & \frac{\gamma}{2} \sin 2\theta_\gamma \\ \frac{\gamma}{2} \sin 2\theta_\gamma & 1 + \frac{\gamma}{2}(1 - \cos 2\theta_\gamma) \end{pmatrix} \begin{pmatrix} \cos \theta & -\sin \theta \\ \sin \theta & \cos \theta \end{pmatrix}, \quad (5)$$

where  $\rho$  is the scale correction factor,  $\theta$  is the difference in orientation angle.  $\gamma$  and  $\theta_\gamma$  describe the shear component by representing respectively the amplitude and orientation angle of a contraction axis. Solving (5) leads to

$$\gamma = \mp \frac{2Y}{X \pm Y}, \quad (6)$$

where

$$X = \sqrt{(A_{11} + A_{22})^2 + (A_{12} - A_{21})^2}, \quad (7)$$

$$Y = \sqrt{(A_{11} - A_{22})^2 + (A_{12} + A_{21})^2}. \quad (8)$$

By imposing  $\gamma \leq 0$  (corresponding to a contraction along some axis, due to atmospheric refraction for instance), it is found:

$$\rho = \frac{X - Y}{2}, \quad (9)$$

$$\gamma = -\frac{2Y}{X - Y}, \quad (10)$$

$$\tan \theta = \frac{A_{21} - A_{12}}{A_{11} + A_{22}}, \quad (11)$$

and

$$\tan 2\theta_\gamma = 2 \frac{A_{11}A_{21} + A_{12}A_{22}}{A_{11}^2 + A_{12}^2 - A_{22}^2 - A_{21}^2}. \quad (12)$$

The CHECKPLOT SHEAR\_VS\_GAMMA allows one to monitor the evolution of  $\gamma$  as a function of airmass.

### 6.7.5 Performance of the matching procedure

The matching performance depends strongly on the depth and reliability of the astrometric reference catalogue. Position angle of the frame and pixel scale can usually be recovered reliably for position uncertainties (POSITION\_MAXERR) about as large as the field of view. If the position angle and pixel scale are already properly set in the image headers, position uncertainties as large as three times the field of view can generally be successfully corrected.

## 6.8 Cross-identification

SCAMP makes heavy use of cross-identification between the various catalogues at several stages of the processing. This process is not totally optimised in the current versions of SCAMP. The tolerance radius (in arcsec) can be changed with the CROSSID\_RADIUS configuration parameter. The default value is presently 2".

## 6.9 Astrometric solution

### 6.9.1 Principle

The astrometric solution is the result of a  $\chi^2$  minimisation. The adopted  $\chi^2$  is the quadratic sum of differences in position between overlapping detections from pairs of fields. One of those fields may be a reference field, or both may be uncalibrated. In both cases, coordinates used in the differences are *reprojected* coordinates  $\xi$ , common to all fields of a same group. The  $\xi$ 's are derived from the measured detector coordinates  $x$ , and the reprojection operator  $\xi(x)$  is different for each field, and even each set. Minimising (13) leads to a solution which adjusts best (in the  $\chi^2$  sense) all the various fields together while tightening the whole group to the reference catalogue:

$$\chi^2 = \sum_s \sum_a \sum_{b>a} w_{s,a,b} \|\xi_a(\mathbf{x}_{s,a}) - \xi_b(\mathbf{x}_{s,b})\|^2, \quad (13)$$

where  $w_{s,a,b}$  is the non-zero weight for the pair of detections in fields  $a$  and  $b$  related to source  $s$ :

$$w_{s,a,b} = \frac{1}{\sigma_{s,a}^2 + \sigma_{s,b}^2}. \quad (14)$$

$\sigma_{s,f}$  is the positional uncertainty for source  $s$  in field  $f$ .

For mosaic cameras, a catalogue comprises several sub-catalogues for each field: one per detector chip. We express the reprojection operator  $\xi_{c,f}$  for chip  $c$  and field  $f$  as a combination of an undistorted reprojection operator  $\xi_{c,f}^0$  derived from the (tangential) projection approximated at the initial matching stage, and two decompositions over linear subspaces describing instrumental distortions as deformations of the pixel grid:

$$\xi_{c,f}(\mathbf{x}) = \xi_{c,f}^0 \left( \mathbf{x} + \sum_p \mathbf{c}_{i,p} \phi_p(\mathbf{o}) + \sum_m \mathbf{d}_{f,m} \psi_m(\boldsymbol{\rho}) \right). \quad (15)$$

Both decompositions The vector  $\chi$  represents the “context” of observation of a given source. The components of  $\mathbf{o}$  may affect the projection distortion at the current position on the field. In general,  $\mathbf{o}$  will include at least the current coordinate vector  $\mathbf{x}$  since distortion on a focal plane is position-dependent. It may also contain field-dependent parameters like airmass or time. The components of the vector  $\mathbf{o}$  are selected using the DISTORT\_KEYS configuration parameter. The arguments can be names of SExtractor measurements, or keywords from the image FITS headers (or .ahead files) representing numerical values. FITS header keywords must be preceded with a colon (:), like in :AIRMASS. The default DISTORT\_KEYS are XWIN\_IMAGE,YWIN\_IMAGE.

The basis functions  $\phi_p$  in the current versions of SCAMP are simple polynomials of the components of  $\chi$ . Each of these components  $\chi_l$  belongs to a “distortion group”  $g = 0, 1, \dots, N_g$ , such that

$$\phi_p(\chi) = \prod_{g < N_g} \left( \prod_{\substack{l \in \Lambda_g \\ (\sum_{l \in \Lambda_g} d_l) \leq D_g}} \chi_l^{d_l} \right), \quad (16)$$

where  $\Lambda_g$  is the set of contexts  $l$  that belongs to the distortion group  $g$ , and  $D_g \in \mathbb{N}$  is the polynomial degree of group  $g$ . Index  $p$  runs over all possible combinations of the  $d_l$  and  $g$ . The DISTORT\_GROUPS configuration parameters in combination with the DISTORT\_KEYS must be filled in to indicate which distortion group each component of  $\chi$  belongs to. The default for DISTORT\_GROUPS is 1,1, meaning that both DISTORT\_KEYS belong to the same unique distortion group. The polynomial degrees  $D_g$  are set with DISTORT\_DEGREES. The default DISTORT\_DEGREES is 3. For most instruments, a 3<sup>rd</sup> degree polynomial is sufficient; one may however consider increasing it to 4 or more for strongly distorted images such as those coming from large FPAs in very-wide field instruments, or photographic plates from Schmidt telescopes. DISTORTION check-plots show maps of the pixel scale over the field of view, and can be useful for checking how the polynomial behaves in every frame (Fig. 7).

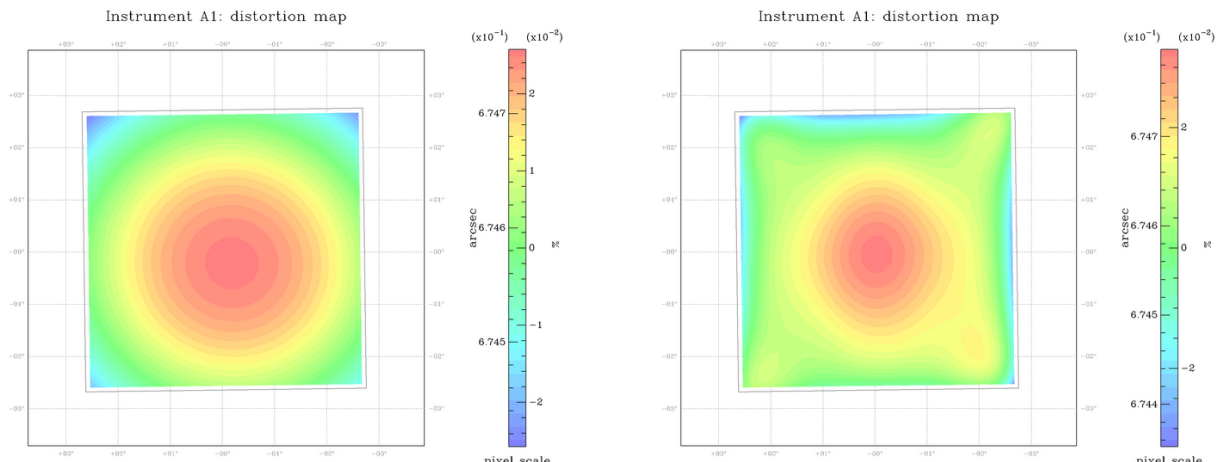


Figure 7: Map of the pixel scale computed by SCAMP on an ESO R Schmidt plate calibrated with a 3<sup>rd</sup> order polynomial (*left*) and a 7<sup>th</sup> order polynomial (*right*): a high-order polynomial allows the pincushion distortion present in this image (Schmidt plate scan courtesy of CAI/Paris observatory) to be modelled properly, and leads to lower astrometric residuals.

The vectors of coefficients  $\mathbf{c}_p$  in (??) are the ones we are looking for. They depend on the detector and the instrument; they can also be made dependent on the current field if the geometry of the instrument is particularly unstable. In SCAMP, this is controlled by the **STABILITY\_TYPE** configuration parameter. Currently supported types for **STABILITY\_TYPE** are

- **EXPOSURE**: allows the astrometric solution to vary for every exposure. Should be used only for geometrically unstable instruments (dismounted and remounted between exposures, with field rotators, etc.)
- **INSTRUMENT**: the astrometric solution for each set is constant for a given instrument. However, linear transformations (scale/rotation/shear and shift, i.e. size degrees of freedom in total for the whole focal plane) are allowed to vary from exposure to exposure, to provide first order corrections for flexures and differential refraction. This is the default behaviour.

For simplicity we assume in the following that the  $\mathbf{c}_p$  do not depend on the field; the mathematical treatment for the full **STABILITY\_TYPE INSTRUMENT** case can be found in Appendix 12.

In general  $\boldsymbol{\xi}^0$  is not a linear operator; it is however expected to be a smooth function of detector coordinates. On the other hand, the success of the pattern matching procedure ensures that  $\boldsymbol{\xi}^0$  is already a fairly good approximation of the exact re-projection, as residual positional errors are a tiny fraction of the field size (typically 1" or less with optical images).  $\boldsymbol{\xi}(\mathbf{x})$  can therefore be approximated with a good accuracy by

$$\boldsymbol{\xi}_f(\mathbf{x}) \approx \boldsymbol{\xi}^0(\mathbf{x}) + \left( \frac{d\boldsymbol{\xi}^0}{d\mathbf{x}} \right)_{\mathbf{x}} (\mathbf{x}' - \mathbf{x}), \quad (17)$$

where  $\left( \frac{d\boldsymbol{\xi}^0}{d\mathbf{x}} \right)_{\mathbf{x}}$  is the Jacobian matrix of the initial re-projection at position  $\mathbf{x}$ :

$$\left[ \left( \frac{d\boldsymbol{\xi}^0}{d\mathbf{x}} \right) \right]_{ij} = \left( \frac{\partial \xi_i^0}{\partial x_j} \right). \quad (18)$$

Incorporating (17) in (13) we obtain

$$\chi^2 = \sum_s \sum_a \sum_{b>a} w_{sab} \left\| \boldsymbol{\xi}_a^0(\mathbf{x}_{sa}) + \left( \frac{d\boldsymbol{\xi}_a^0}{d\mathbf{x}} \right)_{\mathbf{x}_{sa}p} \sum_p \mathbf{c}_p \phi_p(\boldsymbol{\chi}_{sa}) - \boldsymbol{\xi}_b^0(\mathbf{x}_{sb}) - \left( \frac{d\boldsymbol{\xi}_b^0}{d\mathbf{x}} \right)_{\mathbf{x}_{sb}p} \sum_p \mathbf{c}_p \phi_p(\boldsymbol{\chi}_{sb}) \right\|^2, \quad (19)$$

which in scalar form gives

$$\begin{aligned} \chi^2 = \sum_s \sum_a \sum_{b>a} w_{sab} \sum_d & \left( \xi_{ad}^0(\mathbf{x}_{sa}) - \xi_{bd}^0(\mathbf{x}_{sb}) + \sum_e \left( \frac{\partial \xi_{ad}^0}{\partial x_{ae}} \right) \sum_p c_{pe} \phi_p(\boldsymbol{\chi}_{sa}) - \right. \\ & \left. \sum_e \left( \frac{\partial \xi_{bd}^0}{\partial x_{be}} \right) \sum_p c_{pe} \phi_p(\boldsymbol{\chi}_{sb}) \right)^2, \end{aligned} \quad (20)$$

where the  $d$  and  $e$  indices loop over the two axes of the coordinate system. The  $c_{pe}$  are found using  $\chi^2$  minimisation:

$$\frac{\partial \chi^2}{\partial c_{qf}} = 2 \sum_s \sum_a \sum_{b>a} w_{sab}$$

$$\sum_d \left( \xi_{ad}^0(\mathbf{x}_{sa}) - \xi_{bd}^0(\mathbf{x}_{sb}) + \sum_e \left( \frac{\partial \xi_{ad}^0}{\partial x_{ae}} \right)_{\mathbf{x}_{sa}p} c_{pe} \phi_p(\chi_{sa}) - \sum_e \left( \frac{\partial \xi_{bd}^0}{\partial x_{be}} \right)_{\mathbf{x}_{sb}p} c_{pe} \phi_p(\chi_{sb}) \right) \times \\ \left( \left( \frac{\partial \xi_{ad}^0}{\partial x_{af}} \right)_{\mathbf{x}_{sa}} \phi_q(\chi_{sa}) - \left( \frac{\partial \xi_{bd}^0}{\partial x_{bf}} \right)_{\mathbf{x}_{sb}} \phi_q(\chi_{sb}) \right) = 0 \quad \forall q \leq N_q, f = 1, 2, \quad (21)$$

where  $N_q$  is the number of free parameters  $c_{qf}$  in each dimension  $f$ . This leads to the normal equations

$$[\boldsymbol{\alpha}] \cdot \mathbf{c} = \boldsymbol{\beta}, \quad (22)$$

with

$$\alpha_{qf,pe} = \sum_s \sum_a \sum_{b>a} w_{sab} \sum_d \left( \left( \frac{\partial \xi_{ad}^0}{\partial x_{ae}} \right)_{\mathbf{x}_{sa}} \phi_p(\chi_{sa}) - \left( \frac{\partial \xi_{bd}^0}{\partial x_{be}} \right)_{\mathbf{x}_{sb}} \phi_p(\chi_{sb}) \right) \times \\ \left( \left( \frac{\partial \xi_{ad}^0}{\partial x_{af}} \right)_{\mathbf{x}_{sa}} \phi_q(\chi_{sa}) - \left( \frac{\partial \xi_{bd}^0}{\partial x_{bf}} \right)_{\mathbf{x}_{sb}} \phi_q(\chi_{sb}) \right), \quad (23)$$

and

$$\beta_{qe} = \sum_s \sum_a \sum_{b>a} w_{sab} \sum_d (\xi_{bd}^0(\mathbf{x}_{sb}) - \xi_{ad}^0(\mathbf{x}_{sa})) \times \left( \left( \frac{\partial \xi_{ad}^0}{\partial x_{af}} \right)_{\mathbf{x}_{sa}} \phi_q(\chi_{sa}) - \left( \frac{\partial \xi_{bd}^0}{\partial x_{bf}} \right)_{\mathbf{x}_{sb}} \phi_q(\chi_{sb}) \right). \quad (24)$$

In (23) and (24),  $a$  and  $b$  apply to the *observed* source catalogues, which provide only a differential calibration. For detection pairs that involve sources from the astrometric reference field  $o$ , we have  $a = o$ , and (23) reduces to

$$\alpha_{qf,pe} = \sum_s \sum_b w_{sob} \sum_d \left( \frac{\partial \xi_{bd}^0}{\partial x_{be}} \right)_{\mathbf{x}_{sb}} \phi_p(\chi_{sb}) \times \left( \frac{\partial \xi_{bd}^0}{\partial x_{bf}} \right)_{\mathbf{x}_{sb}} \phi_q(\chi_{sb}), \quad (25)$$

and (24)

$$\beta_{qe} = \sum_s \sum_b w_{sob} \sum_d (\xi_{od}^0 - \xi_{bd}^0(\mathbf{x}_{sb})) \times \left( \frac{\partial \xi_{bd}^0}{\partial x_{bf}} \right)_{\mathbf{x}_{sb}} \phi_q(\chi_{sb}). \quad (26)$$

In SCAMP, the normal equation matrix is iteratively filled as detection pairs are scanned. As stated earlier, the  $c_{pe}$  coefficients can be made dependent on the exposure (field) or CCD (set). (23) and (24) are a bit more complicated to handle in such cases, but the procedure remains essentially the same.

### 6.9.2 Balancing the constraints

Astrometric reference catalogues are often vastly sparser and suffer from larger positional “noise” than input catalogues. If not corrected, their contribution to the  $\chi^2$  of (20) may often be too small to properly tighten the solution to the sky, and systematic effects such as bends or ripples may show up in the plots of astrometric residuals. The consequences can be particularly serious in surveys with poorly designed observing strategies (Fig. 8). In SCAMP, the problem is circumvented to some extent by artificially “boosting” the  $w_{sob}$ ’s in (25) and (26) to compensate for the smaller number of detection-reference pairs compared to detection-detection pairs.

Yet this procedure may still be inadequate in some cases, for instance if a catalogue contains a large number of spurious sources or if some positional uncertainties have been grossly under- or over-estimated. Therefore the SCAMP user is given the possibility to apply, if necessary, an additional multiplicative factor to the  $w_{sob}$ ’s in the range of  $10^{-6}$  to  $10^6$  (default is 1.0) using the `ASTREF_WEIGHT` configuration parameter.

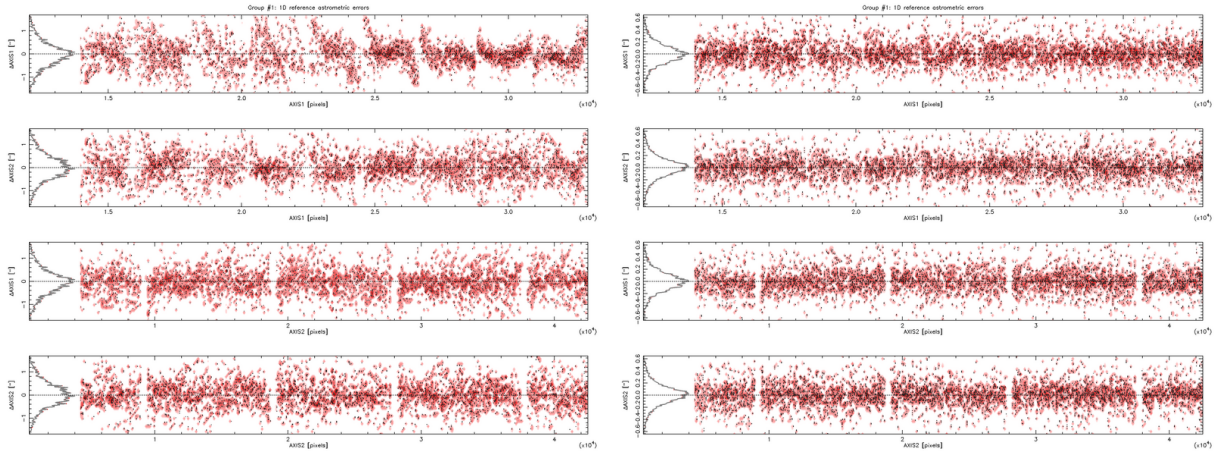


Figure 8: Effect of balancing the weights of source pairs in a sequence of 6 MEGACAM exposures taken with a poorly designed dithering pattern. *Left:* astrometric residuals of the solution without balancing. *Right:* with automatic balancing.

### 6.9.3 Taking care of outliers

Source blending and mismatched detections are the main contributors to the non-Gaussian tails of the position error distribution. Spurious sources, like artifacts of electronic origin, diffraction spikes and halos caused by corrector lenses are also sources of problems. This is why it is important to eliminate as many false detections as possible from the input catalogues prior to running SCAMP by using weight-maps and reasonable threshold levels for source extraction.

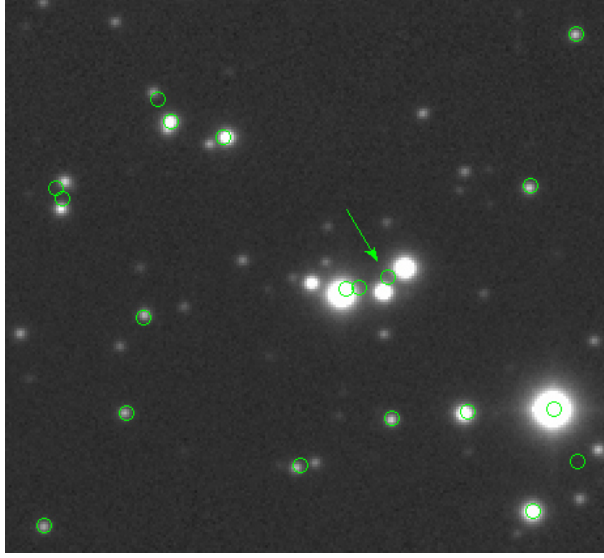


Figure 9: Example of mismatching (indicated by the arrow) between the astrometric reference catalogue (green circles) and the sources present in a CCD image. The mismatch may be caused by stellar proper motions and/or differences in image quality leading to blending of some of the sources in the reference catalogue or in the CCD image.

Cross-matching issues with the reference catalogues are more difficult to solve. Schmidt-plate based reference catalogues (USNO and GSC), in particular, exhibit considerable deblending problems in stellar fields (Fig. 9), leading to “kicks” in the astrometric solution. A removal

of outliers is therefore necessary. In SCAMP a clipping is performed at `ASTRCLIP_NSIGMA` standard deviations after computing a first astrometric solution. For `ASTRCLIP_NSIGMA` = 3.0 (the default), SCAMP eliminates 1 to 3% of sources in typical conditions. After clipping, a new cross-identification is done, and the final astrometric solution is finally computed.

## 6.10 Photometric solution

### 6.11 Photometric measurements

SCAMP requires one flux measurement and its associated uncertainty for every detection. The names of the columns containing both quantities in the input catalogues can be specified with the `PHOTFLUX_KEY` and `PHOTFLUXERR_KEY` configuration parameters, respectively. The kind of flux measurement chosen may have a significant influence on the final photometric calibration. The default measurements are SExtractor’s `FLUX_AUTO` and `FLUXERR_AUTO`. Although these are not the most accurate measurements one can think of, they have the benefit of being rather insensitive to source shapes and changes in image quality from exposure to exposure.

The flux measurements  $f$  are assumed to be in ADUs, that is, in units of pixel values. To allow photometric measurements to be compared between exposures under various observing conditions or even between different instruments, the instrumental fluxes read in the input catalogues are converted to “magnitudes” with

$$m = -2.5 \log_{10} f + m_0 + 2.5 \log t + c_a \cdot a, \quad (27)$$

where  $m_0$  is the instrumental zero-point for a 1 second exposure,  $t$  is the exposure time,  $c_a$  is the extinction coefficient at unit airmass and  $a$  is the average exposure airmass.

#### 6.11.1 Principle

There are some specific issues related to the computation of a photometric solution. In SCAMP, the photometric solution is the result of a  $\chi^2$  minimisation. The adopted  $\chi^2$  is the quadratic sum of differences in magnitude between overlapping detections from pairs of exposures observed with the same photometric instrument.

SCAMP distinguishes between two kinds of exposures: those observed under photometric conditions and the others. “Photometric” exposures must have been calibrated beforehand; they are identified by the photometric flag set to T (true) in their image headers or `.ahead` input files. The FITS keyword associated with the photometric flag can be set with the `PHOTOMFLAG_KEY` configuration parameter. `PHOTFLAG` is the default keyword.

One of those fields may be a photometric field, or both may be uncalibrated. Minimising (28) leads to a solution which adjusts best (in the  $\chi^2$  sense) all the various fields together while tightening the whole group to the photometric field zero-point:

$$\chi^2 = \sum_s \sum_a \sum_{b>a} w_{sa} (Z_a + m_{sa} - Z_b - m_{sb})^2, \quad (28)$$

where  $w_{sa}$  is the non-zero weight for the pair of detections in fields  $a$  and  $b$  related to source  $s$ :

$$w_{sa} = \frac{1}{\sigma_{sa}^2 + \sigma_{sb}^2}. \quad (29)$$

$\sigma_{sf}^2$  is the estimate of magnitude error for source  $s$  in field  $f$ .

The  $Z_a$  are found using  $\chi^2$  minimisation:

$$\frac{\partial \chi^2}{\partial Z_a} = 2 \sum_s \sum_a \sum_{b>a} w_{sab} (Z_a + m_{sa} - Z_b - m_{sb}) = 0. \quad (30)$$

This leads to the normal equations

$$[\boldsymbol{\alpha}] \cdot \mathbf{c} = \boldsymbol{\beta}, \quad (31)$$

TBC

## 6.12 Differential chromatic refraction

Unless an observing filter is infinitely narrow, the average wavelength of the transmitted flux depends on the local slope of the continuum. This small shift in “effective wavelength” translates into a shift of the image if a dispersive device lies in the optical path. The dispersive device can be some refractive optics (i.e. a lens with chromatic aberrations), or the atmosphere at high airmasses. At zenithal angles  $z$  below 80 degrees, the refraction angle is well approximated by

$$\Delta z = R \tan z, \quad (32)$$

where  $R$  is the constant of refraction, which depends exclusively on the refraction index  $n$  at the observing site:

$$R = \frac{n^2 - 2}{2n^2} \approx (n - 1). \quad (33)$$

$n$  is a function of site pressure  $P$  (in hPa), temperature  $T$  (in K), partial vapour pressure  $p_w$  (in hPa) and observing wavelength  $\lambda$  in  $\mu\text{m}$  (Cox, 2000, and references therein):

$$n = 1 + \left( 6.4328 \cdot 10^{-5} + \frac{2.94981 \cdot 10^{-2}}{146 - \lambda^{-2}} + \frac{2.554 \cdot 10^{-4}}{41 - \lambda^{-2}} \right) \cdot \left( \frac{288.15}{T} \right) \cdot \left( \frac{P}{1013.25} \right) - 4.349 \cdot 10^{-5} (1 - 7.956 \cdot 10^{-3} \cdot \lambda^{-2}) \cdot \left( \frac{p_w}{1013.25} \right). \quad (34)$$

Therefore, the tiny shift  $\delta\Delta z$  in arcsec along  $z$  for a small change of wavelength  $\delta\lambda$  around  $\lambda$  can be approximated by

$$\delta\Delta z = \frac{180 \times 3600}{\pi} \frac{dn}{d\lambda} \tan z \delta\lambda \quad (35)$$

$$= \left( \left( \frac{18253}{(146\lambda^2 - 1)^2} + \frac{158.0}{(41\lambda^2 - 1)^2} \right) \cdot \left( \frac{288.15}{T} \right) \cdot \left( \frac{P}{1013.25} \right) \lambda - 0.2141 \left( \frac{p_w}{1013.25} \right) \lambda^{-3} \right) \tan z \delta\lambda. \quad (36)$$

At sea level and at a zenithal distance of 45 degrees,  $\delta\Delta z/\delta\lambda$  varies from about 2 to 15  $"\mu\text{m}^{-1}$  in the optical domain (it is larger at shorter wavelengths).

To compute the effect of differential chromatic refraction on the continuum of a source, we may assume to first order that the instrumental magnitude of the source seen through a filter with an infinitely small bandwidth behaves as a linear function of  $\delta\lambda$ :

$$m(\delta\lambda) = m_0 - \alpha \delta\lambda, \quad (37)$$

where  $\alpha$  is the local slope of the continuum, and can easily be derived from colour indices; the  $\alpha$  of stars lies typically between 0 and  $10 \mu\text{m}^{-1}$  in the optical domain (AB system). The flux density writes

$$f_\nu(\delta\lambda) \propto 10^{0.4 \alpha \delta\lambda} \quad (38)$$

$$\propto e^{0.921 \alpha \delta\lambda}. \quad (39)$$

Now, integrating the flux through a spectral top-hat filter of width  $w$  centred on  $\lambda_0$ , one finds the resulting shift (in arcsec) as a function of  $\alpha$ :

$$\Delta z_{\lambda_0,w}(\alpha) \approx \frac{180 \times 3600}{\pi} \left( \frac{dn}{d\lambda} \right)_{\lambda_0} \tan z \frac{\int_{-w/2}^{+w/2} \delta\lambda f_\nu(\delta\lambda) d\delta\lambda}{\int_{-w/2}^{+w/2} f_\nu(\delta\lambda) d\delta\lambda} \quad (40)$$

$$\approx 206265 \left( \frac{dn}{d\lambda} \right)_{\lambda_0} \tan z \left( \frac{w}{2} \coth \left( 0.921 \frac{w\alpha}{2} \right) - \frac{1}{0.921 \alpha} \right) \quad (41)$$

$$\approx 206265 \left( \frac{dn}{d\lambda} \right)_{\lambda_0} \tan z 0.921 \frac{w^2 \alpha}{8} \quad (42)$$

$$\approx 23750 \left( \frac{dn}{d\lambda} \right)_{\lambda_0} \tan z w^2 \alpha. \quad (43)$$

One can see that at sea level and at a zenithal distance of 45 degrees,  $\Delta z_{\lambda_0,w}$  varies from star to star by about 20 to 150 mas in typical broadband optical filters ( $w \approx 0.1\mu m$ ), depending on the wavelength  $\lambda_0$ . For ground-based observations made at any significant airmass through this kind of filters, there is therefore a small, but often detectable, approximately linear dependency between the measured position of a star and its colour. This effect will be taken into account by SCAMP before computing proper motions on overlaps involving exposures taken with different filters, by fitting a line in a  $\Delta$ -position *vs*  $\Delta$ -magnitude diagram (Fig. 10). It is however impossible for overlapping exposures made at the same wavelengths but with very different airmasses: the result will be an increased dispersion along the average altitude axis.

## 7 Merged output catalogue

In addition to astrometric header information, SCAMP can write out “merged” catalogues (one per field group). These catalogues contain the calibrated coordinates and magnitudes of a union of all detections from input catalogues that passed the SCAMP acceptation criteria (S/N, flags). Merged coordinates and magnitudes are computed using a weighted average of all overlapping measurements, and are accompanied by estimates of formal errors and  $1-\sigma$  uncertainties on individual measurements. Table 2 lists all the columns present in the file.

The `MERGEDOUTCAT_TYPE` configuration parameter sets the format of the merged catalogue; it is set to `NONE` by default, which means that no catalogue is created. The available formats are `ASCII` (pure ASCII table), `ASCII_HEAD` (ASCII table with a small header describing the column content), and `FITS_LDAC` (FITS binary table). `FITS_LDAC` is the recommended format; `FITS_LDAC` files are smaller, carry the data with full precision, and can be read with popular software such as `FV` and `TOPCAT`. They can be converted to ASCII format with the `ldactoasc` command-line utility, which is part of the `SExtractor` package.

## 8 Full output catalogue

Other catalogues which can be produced by SCAMP are the “full” catalogues (one per field group). These catalogues contain the raw and calibrated coordinates and magnitudes of all individual detections that passed the SCAMP acceptation criteria. Each detection is linked to a parent source through to the `SOURCE_NUMBER` identifiant, also present in the merged output catalogue. Table 3 lists all the columns present in the file.

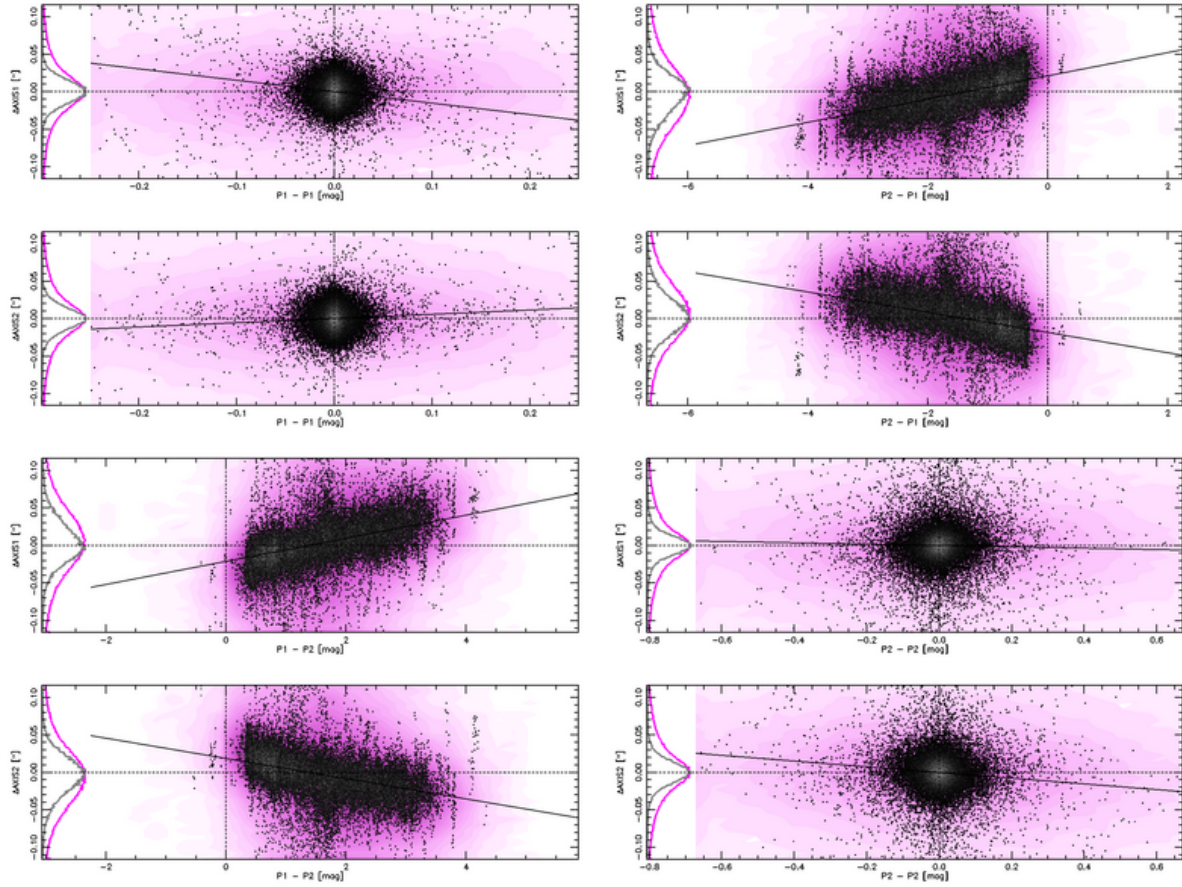


Figure 10: “Check-plot” `ASTR_COLSHIFT1D` showing the internal residuals of the astrometric solution in x and y as a function of magnitude difference for two sets of CFHT-MEGACAM exposures taken at fairly high airmass ( $\approx 1.6$ ). The first set is with the “green”  $g$  filter (labelled here as photometric instrument P1), while the second is with the infrared  $z$  filter (labelled here as photometric instrument P2). Differential chromatic refraction seems to occur along the diagonal direction in the images: this was expected since observations were carried out far from the meridian.

The `FULLOUTCAT_TYPE` configuration parameter sets the format of the full catalogue; the choice of options is the same as for `MERGEDOUTCAT_TYPE`.

## 9 Examples

In the following, examples of use of SCAMP are given, together with commented command lines.

### 9.1 Example 1

TBW

Table 2: List of parameters written to the merged output catalogue

| Name              | Content   | Unit   |
|-------------------|---|--------|
| SOURCE_NUMBER     | Source ID   | -      |
| NPOS_TOTAL        | Total number of overlapping positions                             | -      |
| NPOS_OK           | Number of overlapping positions kept for astrometry               | -      |
| ALPHA_J2000       | (Weighted-)average Right-Ascension                                | deg    |
| DELTA_J2000       | (Weighted-)average Declination                                    | deg    |
| ERRA_WORLD        | Position uncertainty (RMS) along major world axis                 | deg    |
| ERRB_WORLD        | Position uncertainty (RMS) along minor world axis                 | deg    |
| ERRTHETA_WORLD    | Position angle of error ellipse <sup>a</sup> (CCW/world-x)        | deg    |
| DISPALPHA_J2000   | Measured dispersion (RMS) of position along Right-Ascension       | deg    |
| DISPDELTJA_J2000  | Measured dispersion (RMS) of position along Declination           | deg    |
| PMALPHA_J2000     | Apparent proper motion along Right-Ascension                      | mas/yr |
| PMDELTA_J2000     | Apparent proper motion along Declination                          | mas/yr |
| PMALPHAERR_J2000  | Proper motion uncertainty (RMS) along Right Ascension             | mas/yr |
| PMDELTAERR_J2000  | Proper motion uncertainty (RMS) along Declination                 | mas/yr |
| PARALLAX_WORLD    | Trigonometric parallax  | mas    |
| PARALLAXERR_WORLD | Trigonometric parallax uncertainty                                | mas    |
| CHI2_ASTROM       | Reduced $\chi^2$ per d.o.f. of the proper motion/parallax fit     | -      |
| EPOCH             | (Astrometrically-)weighted-average of observation dates           | yr     |
| EPOCH_MIN         | Earliest observation date   | yr     |
| EPOCH_MAX         | Latest observation date   | yr     |
| NMAG              | Number of magnitude measurements in each “photometric instrument” | -      |
| MAG               | Vector of (flux-weighted-)average magnitudes                      | mag    |
| MAGERR            | Vector of magnitude uncertainties                                 | mag    |
| MAG_DISP          | Vector of measured magnitude dispersions (RMS)                    | mag    |
| COLOR             | Composite colour index computed by SCAMP                          | mag    |
| SPREAD_MODEL      | (Weighted-)average of SPREAD_MODELS                               | -      |
| SPREADERR_MODEL   | SPREAD_MODEL uncertainty  | -      |
| FLAGS_EXTRACTION  | Arithmetic OR of SExtractor flags over overlapping detections     | -      |
| FLAGS_SCAMP       | SCAMP flags for this source                                       | -      |

<sup>a</sup>The current estimation of error ellipse parameters is still done very crudely.

## 9.2 Example 2

TBW

# 10 Troubleshooting

### My window terminal crashes during a long SCAMP run!

Unexpected crashes of XTERM windows have been reported. This seems to be caused by the large number of ANSI control sequences that SCAMP sends to the terminal. You may either set the SCAMP configuration keyword VERBOSE\_TYPE to QUIET, LOG or FULL, and/or redirect the output to a file.

SCAMP crashes with error messages like “> \*Error\*: Not enough memory for...”.

The maximum value allowed by your shell for memory use might be set too low. Use the shell command limit to increase the datasize, memoryuse and vmemoryuse parameters if required (you might need the root privileges to change this if it is a “hard” limit).

For tips and troubleshooting please visit the *AstrOmatic* forum at <http://astromatic.net/forum>.

Table 3: List of parameters written to the full output catalogue

| Name             | Content  | Unit  |
|------------------|--|-------|
| SOURCE_NUMBER    | Source ID  | -     |
| CATALOG_NUMBER   | Catalogue ID   | -     |
| EXTENSION        | FITS extension of the parent image   | -     |
| ASTR_INSTRUM     | Astrometric instrument (context) ID  | -     |
| PHOT_INSTRUM     | Photometric instrument (context) ID  | -     |
| X_IMAGE          | $x$ pixel coordinate of centroid   | pixel |
| Y_IMAGE          | $y$ pixel coordinate of centroid   | pixel |
| ERRA_IMAGE       | Position uncertainty (RMS) along major error ellipse axis                    | pixel |
| ERRB_IMAGE       | Position uncertainty (RMS) along minor error ellipse axis                    | pixel |
| ERRTHETA_IMAGE   | Position angle of error ellipse <sup>a</sup>                                 | deg   |
| ALPHA_J2000      | Calibrated Right-Ascension of centroid in the ICRS (at epoch of observation) | deg   |
| DELTA_J2000      | Calibrated Declination of centroid in the ICRS (at epoch of observation)     | deg   |
| ERRA_WORLD       | Position uncertainty (RMS) along major world axis <sup>b</sup>               | deg   |
| ERRB_WORLD       | Position uncertainty (RMS) along minor world axis <sup>b</sup>               | deg   |
| ERRTHETA_WORLD   | Position angle of error ellipse <sup>c</sup> (CCW/world-x)                   | deg   |
| EPOCH            | Julian date at start of observation  | yr    |
| MAG              | Calibrated magnitude   | mag   |
| MAGERR           | Magnitude uncertainty <sup>b</sup>   | mag   |
| MAG_DISP         | Vector of measured magnitude dispersions (RMS)                               | mag   |
| SPREAD_MODEL     | SPREAD_MODEL parameter   | -     |
| SPREADERR_MODEL  | SPREAD_MODEL uncertainty   | -     |
| FLAGS_EXTRACTION | SEextractor flags  | -     |
| FLAGS_SCAMP      | SCAMP flags for this detection   | -     |

<sup>a</sup>Forced to 0 by current versions of SCAMP which “isotropise” input uncertainties.

<sup>b</sup>may include additional uncertainty computed by SCAMP.

<sup>c</sup>The current estimation of error ellipse parameters is still done very crudely.

## 11 Acknowledging SCAMP

Please use the following reference: **Bertin E.**, 2006, in *Astronomical Data Analysis Software and Systems XV*, ASP Conf. Series **351**, 112.

If you used the built-in access to astrometric catalogues for your research work, please add the following acknowledgement text: “This research has made use of the VizieR catalogue access tool, CDS, Strasbourg, France”.

## 12 Acknowledgements

Many thanks to Florence Durret for her comments on the manuscript, Mark Calabretta for his great astrometric library, François Ochsenbein at CDS for his help with CDSclient, Jan Kohnert for providing focal plane models, Akim Demaille for his help with the autotools, John Moustakas for adding SDSS support, Hervé Bouy for his contributions to the proper motion module and the measurement of atmosphere-induced differential stellar motions, Mireille Dantel, Laurent Domisse, Patrick Hudelot, Jean-Christophe Malapert, Chiara Marmo, Jean-Baptiste Marquette, Yannick Mellier, Henry Joy McCracken and Mario Radovich at IAP, Eric Aubourg at CEA, Jean-Charles Cuillandre at CFHT, Bob Armstrong and Shantanu Desai at U. of Illinois, Wayne Barkhouse, Daniel Durand, Pascal Fouqué, J.P. McFarland, Abhishek Rawat and the AstrOmatic.net forum members for extensive testing and suggestions.

*The Guide Star Catalog-I was produced at the Space Telescope Science Institute under U.S. Government grant. These data are based on photographic data obtained using the Oschin Schmidt Telescope on Palomar Mountain and the UK Schmidt Telescope.*

*The Guide Star Catalogue-II is a joint project of the Space Telescope Science Institute and the Osservatorio Astronomico di Torino. Space Telescope Science Institute is operated by the Association of Universities for Research in Astronomy, for the National Aeronautics and Space Administration under contract NAS5-26555. The participation of the Osservatorio Astronomico di Torino is supported by the Italian Council for Research in Astronomy. Additional support is provided by European Southern Observatory, Space Telescope European Coordinating Facility, the International GEMINI project and the European Space Agency Astrophysics Division.*

*This software makes use of data products from the Two Micron All Sky Survey, which is a joint project of the University of Massachusetts and the Infrared Processing and Analysis Center/California Institute of Technology, funded by the National Aeronautics and Space Administration and the National Science Foundation*

*Funding for the SDSS and SDSS-II has been provided by the Alfred P. Sloan Foundation, the Participating Institutions, the National Science Foundation, the U.S. Department of Energy, the National Aeronautics and Space Administration, the Japanese Monbukagakusho, the Max Planck Society, and the Higher Education Funding Council for England. The SDSS Web Site is <http://www.sdss.org/>*

*The SDSS is managed by the Astrophysical Research Consortium for the Participating Institutions. The Participating Institutions are the American Museum of Natural History, Astrophysical Institute Potsdam, University of Basel, Cambridge University, Case Western Reserve University, University of Chicago, Drexel University, Fermilab, the Institute for Advanced Study, the Japan Participation Group, Johns Hopkins University, the Joint Institute for Nuclear Astrophysics, the Kavli Institute for Particle Astrophysics and Cosmology, the Korean Scientist Group, the Chinese Academy of Sciences (LAMOST), Los Alamos National Laboratory, the Max-Planck-Institute for Astronomy (MPA), the Max-Planck-Institute for Astrophysics (MPIA), New Mexico State University, Ohio State University, University of Pittsburgh, University of Portsmouth, Princeton University, the United States Naval Observatory, and the University of Washington.*

*Funding for SDSS-III has been provided by the Alfred P. Sloan Foundation, the Participating Institutions, the National Science Foundation, and the U.S. Department of Energy Office of Science. The SDSS-III web site is <http://www.sdss3.org/>.*

*SDSS-III is managed by the Astrophysical Research Consortium for the Participating Institutions of the SDSS-III Collaboration including the University of Arizona, the Brazilian Participation Group, Brookhaven National Laboratory, University of Cambridge, Carnegie Mellon University, University of Florida, the French Participation Group, the German Participation Group, Harvard University, the Instituto de Astrofisica de Canarias, the Michigan State/Notre Dame/JINA Participation Group, Johns Hopkins University, Lawrence Berkeley National Laboratory, Max Planck Institute for Astrophysics, Max Planck Institute for Extraterrestrial Physics, New Mexico State University, New York University, Ohio State University, Pennsylvania State University, University of Portsmouth, Princeton University, the Spanish Participation Group, University of Tokyo, University of Utah, Vanderbilt University, University of Virginia, University of Washington, and Yale University.*

*This software makes use of the USNOFS Image and Catalogue Archive operated by the United States Naval Observatory, Flagstaff Station*

*This software makes use of the DeNIS database, which is the result of a joint effort involving human and financial contributions of several Institutes mostly located in Europe. It has been supported financially mainly by the French Institut National des Sciences de l'Univers, CNRS, and French Education Ministry, the European Southern Observatory, the State of Baden-Wuerttemberg, and the European Commission under networks of the SCIENCE and Human Capital and Mobility programs, the Landessternwarte, Heidelberg and Institut d'Astrophysique de Paris.*

## References

- Abazajian K., Adelman-McCarthy J. K., Agüeros M. A., Allam S. S., Anderson K. S. J., Anderson S. F., Annis J., Bahcall N. A., Baldry I. K., Bastian S., Berlind A., Bernardi M., Blanton M. R., Bochanski Jr. J. J., Boroski W. N., Brewington H. J., Briggs J. W., Brinkmann J., Brunner R. J., Budavári T., Carey L. N., Castander F. J., Connolly A. J., Covey K. R., Csabai I., Dalcanton J. J., Doi M., Dong F., Eisenstein D. J., Evans M. L., Fan X., Finkbeiner D. P., Friedman S. D., Frieman J. A., Fukugita M., Gillespie B., Glazebrook K., Gray J., Grebel E. K., Gunn J. E., Gurbani V. K., Hall P. B., Hamabe M., Harbeck D., Harris F. H., Harris

H. C., Harvanek M., Hawley S. L., Hayes J., Heckman T. M., Hendry J. S., Hennessy G. S., Hindsley R. B., Hogan C. J., Hogg D. W., Holmgren D. J., Holtzman J. A., Ichikawa S.-i., Ichikawa T., Ivezić Ž., Jester S., Johnston D. E., Jorgensen A. M., Jurić M., Kent S. M., Kleinman S. J., Knapp G. R., Kniazev A. Y., Kron R. G., Krzesinski J., Lamb D. Q., Lampeitl H., Lee B. C., Lin H., Long D. C., Loveday J., Lupton R. H., Mannery E., Margon B., Martínez-Delgado D., Matsubara T., McGehee P. M., McKay T. A., Meiksin A., Ménard B., Munn J. A., Nash T., Neilsen Jr. E. H., Newberg H. J., Newman P. R., Nichol R. C., Nicinski T., Nieto-Santisteban M., Nitta A., Okamura S., O'Mullane W., Owen R., Padmanabhan N., Pauls G., Peoples J., Pier J. R., Pope A. C., Pourbaix D., Quinn T. R., Raddick M. J., Richards G. T., Richmond M. W., Rix H.-W., Rockosi C. M., Schlegel D. J., Schneider D. P., Schroeder J., Scranton R., Sekiguchi M., Sheldon E., Shimasaku K., Silvestri N. M., Smith J. A., Smolčić V., Snedden S. A., Stebbins A., Stoughton C., Strauss M. A., SubbaRao M., Szalay A. S., Szapudi I., Szkody P., Szokoly G. P., Tegmark M., Teodoro L., Thakar A. R., Tremonti C., Tucker D. L., Uomoto A., Vanden Berk D. E., Vandenberg J., Vogeley M. S., Voges W., Vogt N. P., Walkowicz L. M., Wang S.-i., Weinberg D. H., West A. A., White S. D. M., Wilhite B. C., Xu Y., Yanny B., Yasuda N., Yip C.-W., Yocom D. R., York D. G., Zehavi I., Zibetti S., Zucker D. B., *The Third Data Release of the Sloan Digital Sky Survey*, 2005, AJ, 129, 1755

Abazajian K. N., Adelman-McCarthy J. K., Agüeros M. A., Allam S. S., Allende Prieto C., An D., Anderson K. S. J., Anderson S. F., Annis J., Bahcall N. A., et al., *The Seventh Data Release of the Sloan Digital Sky Survey*, 2009, ApJS, 182, 543

Adelman-McCarthy J. K., Agüeros M. A., Allam S. S., Allende Prieto C., Anderson K. S. J., Anderson S. F., Annis J., Bahcall N. A., Bailer-Jones C. A. L., Baldry I. K., Barentine J. C., Bassett B. A., Becker A. C., Beers T. C., Bell E. F., Berlind A. A., Bernardi M., Blanton M. R., Bochanski J. J., Boroski W. N., Brinchmann J., Brinkmann J., Brunner R. J., Budavári T., Carliles S., Carr M. A., Castander F. J., Cinabro D., Cool R. J., Covey K. R., Csabai I., Cunha C. E., Davenport J. R. A., Dilday B., Doi M., Eisenstein D. J., Evans M. L., Fan X., Finkbeiner D. P., Friedman S. D., Frieman J. A., Fukugita M., Gänsicke B. T., Gates E., Gillespie B., Glazebrook K., Gray J., Grebel E. K., Gunn J. E., Gurbani V. K., Hall P. B., Harding P., Harvanek M., Hawley S. L., Hayes J., Heckman T. M., Hendry J. S., Hindsley R. B., Hirata C. M., Hogan C. J., Hogg D. W., Hyde J. B., Ichikawa S.-i., Ivezić Ž., Jester S., Johnson J. A., Jorgensen A. M., Jurić M., Kent S. M., Kessler R., Kleinman S. J., Knapp G. R., Kron R. G., Krzesinski J., Kuropatkin N., Lamb D. Q., Lampeitl H., Lebedeva S., Lee Y. S., Leger R. F., Lépine S., Lima M., Lin H., Long D. C., Loomis C. P., Loveday J., Lupton R. H., Malanushenko O., Malanushenko V., Mandelbaum R., Margon B., Marriner J. P., Martínez-Delgado D., Matsubara T., McGehee P. M., McKay T. A., Meiksin A., Morrison H. L., Munn J. A., Nakajima R., Neilsen Jr. E. H., Newberg H. J., Nichol R. C., Nicinski T., Nieto-Santisteban M., Nitta A., Okamura S., Owen R., Oyaizu H., Padmanabhan N., Pan K., Park C., Peoples Jr. J., Pier J. R., Pope A. C., Purger N., Raddick M. J., Re Fiorentin P., Richards G. T., Richmond M. W., Riess A. G., Rix H.-W., Rockosi C. M., Sako M., Schlegel D. J., Schneider D. P., Schreiber M. R., Schwope A. D., Seljak U., Sesar B., Sheldon E., Shimasaku K., Sivarani T., Smith J. A., Snedden S. A., Steinmetz M., Strauss M. A., SubbaRao M., Suto Y., Szalay A. S., Szapudi I., Szkody P., Tegmark M., Thakar A. R., Tremonti C. A., Tucker D. L., Uomoto A., Vanden Berk D. E., Vandenberg J., Vidrih S., Vogeley M. S., Voges W., Vogt N. P., Wadadekar Y., Weinberg D. H., West A. A., White S. D. M., Wilhite B. C., Yanny B., Yocom D. R., York D. G., Zehavi I., Zucker D. B., *The Sixth Data Release of the Sloan Digital Sky Survey*, 2008, ApJS, 175, 297

Adelman-McCarthy J. K., Agüeros M. A., Allam S. S., Anderson K. S. J., Anderson S. F., Annis

J., Bahcall N. A., Bailer-Jones C. A. L., Baldry I. K., Barentine J. C., Beers T. C., Belokurov V., Berlind A., Bernardi M., Blanton M. R., Bochanski J. J., Boroski W. N., Bramich D. M., Brewington H. J., Brinchmann J., Brinkmann J., Brunner R. J., Budavári T., Carey L. N., Carliles S., Carr M. A., Castander F. J., Connolly A. J., Cool R. J., Cunha C. E., Csabai I., Dalcanton J. J., Doi M., Eisenstein D. J., Evans M. L., Evans N. W., Fan X., Finkbeiner D. P., Friedman S. D., Frieman J. A., Fukugita M., Gillespie B., Gilmore G., Glazebrook K., Gray J., Grebel E. K., Gunn J. E., de Haas E., Hall P. B., Harvanek M., Hawley S. L., Hayes J., Heckman T. M., Hendry J. S., Hennessy G. S., Hindsley R. B., Hirata C. M., Hogan C. J., Hogg D. W., Holtzman J. A., Ichikawa S.-i., Ichikawa T., Ivezić Ž., Jester S., Johnston D. E., Jorgensen A. M., Jurić M., Kauffmann G., Kent S. M., Kleinman S. J., Knapp G. R., Kniazev A. Y., Kron R. G., Krzesinski J., Kuropatkin N., Lamb D. Q., Lampeitl H., Lee B. C., Leger R. F., Lima M., Lin H., Long D. C., Loveday J., Lupton R. H., Mandelbaum R., Margon B., Martínez-Delgado D., Matsubara T., McGehee P. M., McKay T. A., Meiksin A., Munn J. A., Nakajima R., Nash T., Neilsen Jr. E. H., Newberg H. J., Nichol R. C., Nieto-Santisteban M., Nitta A., Oyaizu H., Okamura S., Ostriker J. P., Padmanabhan N., Park C., Peoples Jr. J., Pier J. R., Pope A. C., Pourbaix D., Quinn T. R., Raddick M. J., Re Fiorentin P., Richards G. T., Richmond M. W., Rix H.-W., Rockosi C. M., Schlegel D. J., Schneider D. P., Scranton R., Seljak U., Sheldon E., Shimasaku K., Silvestri N. M., Smith J. A., Smolčić V., Snedden S. A., Stebbins A., Stoughton C., Strauss M. A., SubbaRao M., Suto Y., Szalay A. S., Szapudi I., Szkody P., Tegmark M., Thakar A. R., Tremonti C. A., Tucker D. L., Uomoto A., Vanden Berk D. E., Vandenberg J., Vidrih S., Vogeley M. S., Voges W., Vogt N. P., Weinberg D. H., West A. A., White S. D. M., Wilhite B., Yanny B., Yocom D. R., York D. G., Zehavi I., Zibetti S., Zucker D. B., The Fifth Data Release of the Sloan Digital Sky Survey, 2007, ApJS, 172, 634

Ahn C. P., Alexandroff R., Allende Prieto C., Anderson S. F., Anderton T., Andrews B. H., Aubourg É., Bailey S., Balbinot E., Barnes R., et al., The Ninth Data Release of the Sloan Digital Sky Survey: First Spectroscopic Data from the SDSS-III Baryon Oscillation Spectroscopic Survey, 2012, ApJS, 203, 21

Aihara H., Allende Prieto C., An D., Anderson S. F., Aubourg É., Balbinot E., Beers T. C., Berlind A. A., Bickerton S. J., Bizyaev D., Blanton M. R., Bochanski J. J., Bolton A. S., Bovy J., Brandt W. N., Brinkmann J., Brown P. J., Brownstein J. R., Busca N. G., Campbell H., Carr M. A., Chen Y., Chiappini C., Comparat J., Connolly N., Cortes M., Croft R. A. C., Cuesta A. J., da Costa L. N., Davenport J. R. A., Dawson K., Dhital S., Ealet A., Ebelke G. L., Edmondson E. M., Eisenstein D. J., Escoffier S., Esposito M., Evans M. L., Fan X., Femenía Castellá B., Font-Ribera A., Frinchaboy P. M., Ge J., Gillespie B. A., Gilmore G., González Hernández J. I., Gott J. R., Gould A., Grebel E. K., Gunn J. E., Hamilton J.-C., Harding P., Harris D. W., Hawley S. L., Hearty F. R., Ho S., Hogg D. W., Holtzman J. A., Honscheid K., Inada N., Ivans I. I., Jiang L., Johnson J. A., Jordan C., Jordan W. P., Kazin E. A., Kirkby D., Klaene M. A., Knapp G. R., Kneib J.-P., Kochanek C. S., Koesterke L., Kollmeier J. A., Kron R. G., Lampeitl H., Lang D., Le Goff J.-M., Lee Y. S., Lin Y.-T., Long D. C., Loomis C. P., Lucatello S., Lundgren B., Lupton R. H., Ma Z., MacDonald N., Mahadevan S., Maia M. A. G., Makler M., Malanushenko E., Malanushenko V., Mandelbaum R., Maraston C., Margala D., Masters K. L., McBride C. K., McGehee P. M., McGreer I. D., Ménard B., Miralda-Escudé J., Morrison H. L., Mullally F., Muna D., Munn J. A., Murayama H., Myers A. D., Naugle T., Neto A. F., Nguyen D. C., Nichol R. C., O’Connell R. W., Ogando R. L. C., Olmstead M. D., Oravetz D. J., Padmanabhan N., Palanque-Delabrouille N., Pan K., Pandey P., Pâris I., Percival W. J., Petitjean P., Pfaffenberger R., Pforr J., Phleps S., Pichon C., Pieri M. M., Prada F., Price-Whelan A. M., Raddick M. J., Ramos B. H. F., Reylé C., Rich J., Richards G. T., Rix H.-W., Robin A. C., Rocha-Pinto H. J., Rockosi C. M.,

Roe N. A., Rollinde E., Ross A. J., Ross N. P., Rossetto B. M., Sánchez A. G., Sayres C., Schlegel D. J., Schlesinger K. J., Schmidt S. J., Schneider D. P., Sheldon E., Shu Y., Simmerer J., Simmons A. E., Sivarani T., Snedden S. A., Sobeck J. S., Steinmetz M., Strauss M. A., Szalay A. S., Tanaka M., Thakar A. R., Thomas D., Tinker J. L., Tofflemire B. M., Tojeiro R., Tremonti C. A., Vandenberg J., Vargas Magaña M., Verde L., Vogt N. P., Wake D. A., Wang J., Weaver B. A., Weinberg D. H., White M., White S. D. M., Yanny B., Yasuda N., Yeh C., Zehavi I., *The Eighth Data Release of the Sloan Digital Sky Survey: First Data from SDSS-III*, 2011, ApJS, 193, 29

Copenhagen University O., Institute A. O., Cambridge, Uk, Real Instituto Y Observatorio de La Armada F. E. S., Carlsberg Meridian Catalog 14 (CMC14) (CMC, 2006)., 2006, VizieR Online Data Catalog, 1304, 0

Cox A. N., 2000, Allen's astrophysical quantities

Cutri R. M., Skrutskie M. F., van Dyk S., Beichman C. A., Carpenter J. M., Chester T., Cambresy L., Evans T., Fowler J., Gizis J., Howard E., Huchra J., Jarrett T., Kopan E. L., Kirkpatrick J. D., Light R. M., Marsh K. A., McCallon H., Schneider S., Stiening R., Sykes M., Weinberg M., Wheaton W. A., Wheelock S., Zacarias N., 2MASS All-Sky Catalog of Point Sources (Cutri+ 2003), 2003, VizieR Online Data Catalog, 2246, 0

DENIS Consortium, The DENIS database (DENIS Consortium, 2005), 2005, VizieR Online Data Catalog, 2263, 0

Han I., Gatewood G. D., A Study of the Accuracy of Narrow Field Astrometry using Star Trails taken with the CFHT, 1995, PASP, 107, 399

Høg E., Fabricius C., Makarov V. V., Urban S., Corbin T., Wycoff G., Bastian U., Schwerkendiek P., Wicenec A., The Tycho-2 catalogue of the 2.5 million brightest stars, 2000, A&A, 355, L27

Jenkner H., Lasker B. M., Sturch C. R., McLean B. J., Shara M. M., Russel J. L., The Guide Star Catalog. III - Production, database organization, and population statistics, 1990, AJ, 99, 2082

Kaiser N., Wilson G., Luppino G., Dahle H., A Photometric Study of the Supercluster MS0302 with the UH8K CCD Camera: Image Processing and Object Catalogs, 1999, ArXiv Astrophysics e-prints

Lasker B. M., Lattanzi M. G., McLean B. J., Bucciarelli B., Drimmel R., Garcia J., Greene G., Guglielmetti F., Hanley C., Hawkins G., Laidler V. G., Loomis C., Meakes M., Mignani R., Morbidelli R., Morrison J., Pannunzio R., Rosenberg A., Sarasso M., Smart R. L., Spagna A., Sturch C. R., Volpicelli A., White R. L., Wolfe D., Zacchei A., The Second-Generation Guide Star Catalog: Description and Properties, 2008, AJ, 136, 735

Lasker B. M., Sturch C. R., McLean B. J., Russell J. L., Jenkner H., Shara M. M., The Guide Star Catalog. I - Astronomical foundations and image processing, 1990, AJ, 99, 2019

Monet D., 1998, USNO-A2.0

Monet D., Canzian B., Harris H., Reid N., Rhodes A., Sell S., The PMM USNO-A1.0 Catalogue (Monet 1997), 1998, VizieR Online Data Catalog, 1243, 0

Monet D. G., Levine S. E., Canzian B., Ables H. D., Bird A. R., Dahn C. C., Guetter H. H., Harris H. C., Henden A. A., Leggett S. K., Levison H. F., Luginbuhl C. B., Martini J., Monet A. K. B., Munn J. A., Pier J. R., Rhodes A. R., Riepe B., Sell S., Stone R. C., Vrba F. J., Walker R. L., Westerhout G., Brucato R. J., Reid I. N., Schoening W., Hartley M., Read M. A., Tritton S. B., The USNO-B Catalog, 2003, AJ, 125, 984

Morrison J. E., Röser S., McLean B., Buccarelli B., Lasker B., The Guide Star Catalog, Version 1.2: An Astrometric Recalibration and Other Refinements, 2001, AJ, 121, 1752

Ochsenbein F., Bauer P., Marcout J., The VizieR database of astronomical catalogues, 2000, A&AS, 143, 23

Röser S., Schilbach E., Schwan H., Kharchenko N. V., Piskunov A. E., Scholz R.-D., PPM-Extended (PPMX) - a catalogue of positions and proper motions, 2008, A&A, 488, 401

Russell J. L., Lasker B. M., McLean B. J., Sturch C. R., Jenkner H., The Guide Star Catalog. II - Photometric and astrometric models and solutions, 1990, AJ, 99, 2059

Zacharias N., Finch C., Girard T., Hambly N., Wycoff G., Zacharias M. I., Castillo D., Corbin T., DiVittorio M., Dutta S., Gaume R., Gauss S., Germain M., Hall D., Hartkopf W., Hsu D., Holdenried E., Makarov V., Martinez M., Mason B., Monet D., Rafferty T., Rhodes A., Siemers T., Smith D., Tillemann T., Urban S., Wieder G., Winter L., Young A., The Third US Naval Observatory CCD Astrograph Catalog (UCAC3), 2010, AJ, 139, 2184

Zacharias N., Finch C. T., Girard T. M., Henden A., Bartlett J. L., Monet D. G., Zacharias M. I., UCAC4 Catalogue (Zacharias+, 2012), 2012, VizieR Online Data Catalog, 1322, 0

Zacharias N., Monet D. G., Levine S. E., Urban S. E., Gaume R., Wycoff G. L., The Naval Observatory Merged Astrometric Dataset (NOMAD), 2004a, in Bulletin of the American Astronomical Society, Vol. 36, American Astronomical Society Meeting Abstracts, p. 1418

Zacharias N., Urban S. E., Zacharias M. I., Hall D. M., Wycoff G. L., Rafferty T. J., Germain M. E., Holdenried E. R., Pohlman J. W., Gauss F. S., Monet D. G., Winter L., The First US Naval Observatory CCD Astrograph Catalog, 2000, AJ, 120, 2131

Zacharias N., Urban S. E., Zacharias M. I., Wycoff G. L., Hall D. M., Monet D. G., Rafferty T. J., The Second US Naval Observatory CCD Astrograph Catalog (UCAC2), 2004b, AJ, 127, 3043

## Appendix A

This section presents the full mathematical treatment of the STABILITY\_TYPE INSTRUMENT case, including exposure-dependent terms. By adding exposure dependent coefficients  $d_{fm}$  (where  $f$  is the exposure, or “field”), to the  $\mathbf{c}_p$  coefficients (??) becomes

$$\mathbf{x}'_f = \mathbf{x}_f + \sum_p \mathbf{c}_p \phi_p(\chi_f) + \sum_m \mathbf{d}_{fm} \psi_m(\chi_f) \quad (44)$$

$$\begin{aligned} \chi^2 = \sum_s \sum_a \sum_{b>a} w_{sab} \left\| \boldsymbol{\xi}_a^0(\mathbf{x}_{sa}) + \left( \frac{d\boldsymbol{\xi}_a^0}{d\mathbf{x}} \right)_{\mathbf{x}_{sa}} \left( \sum_p \mathbf{c}_p \phi_p(\chi_{sa}) + \sum_m \mathbf{d}_{am} \psi_m(\chi_{sa}) \right) - \right. \\ \left. \boldsymbol{\xi}_b^0(\mathbf{x}_{sb}) - \left( \frac{d\boldsymbol{\xi}_b^0}{d\mathbf{x}} \right)_{\mathbf{x}_{sb}} \left( \sum_p \mathbf{c}_p \phi_p(\chi_{sb}) + \sum_m \mathbf{d}_{bm} \psi_m(\chi_{sb}) \right) \right\|^2, \end{aligned} \quad (45)$$

which in scalar form gives

$$\chi^2 = \sum_s \sum_a \sum_{b>a} w_{sab} \sum_d \left( \xi_{ad}^0(\boldsymbol{x}_{sa}) - \xi_{bd}^0(\boldsymbol{x}_{sb}) + \sum_e \left( \frac{\partial \xi_{ad}^0}{\partial x_{ae}} \right)_{\boldsymbol{x}_{sa}} \left( \sum_p c_{pe} \phi_p(\boldsymbol{\chi}_{sa}) + \sum_m d_{ame} \psi_m(\boldsymbol{\chi}_{sa}) \right) - \sum_e \left( \frac{\partial \xi_{bd}^0}{\partial x_{be}} \right)_{\boldsymbol{x}_{sb}} \left( \sum_p c_{pe} \phi_p(\boldsymbol{\chi}_{sb}) + \sum_m d_{bme} \psi_m(\boldsymbol{\chi}_{sb}) \right) \right)^2, \quad (46)$$

where the  $d$  and  $e$  indices loop over the two axes of the coordinate system. The  $c_{pe}$  and  $d_{bme}$  are found using  $\chi^2$  minimization:

$$\begin{aligned} \frac{\partial \chi^2}{\partial c_{qf}} = & 2 \sum_s \sum_a \sum_{b>a} w_{sab} \sum_d (\xi_{ad}^0(\boldsymbol{x}_{sa}) - \xi_{bd}^0(\boldsymbol{x}_{sb}) + \\ & \sum_e \left( \frac{\partial \xi_{ad}^0}{\partial x_{ae}} \right)_{\boldsymbol{x}_{sa}} \left( \sum_p c_{pe} \phi_p(\boldsymbol{\chi}_{sa}) + \sum_m d_{ame} \psi_m(\boldsymbol{\chi}_{sa}) \right) - \\ & \sum_e \left( \frac{\partial \xi_{bd}^0}{\partial x_{be}} \right)_{\boldsymbol{x}_{sb}} \left( \sum_p c_{pe} \phi_p(\boldsymbol{\chi}_{sb}) + \sum_m d_{bme} \psi_m(\boldsymbol{\chi}_{sb}) \right)) \times \\ & \left( \left( \frac{\partial \xi_{ad}^0}{\partial x_{af}} \right)_{\boldsymbol{x}_{sa}} \phi_q(\boldsymbol{\chi}_{sa}) - \left( \frac{\partial \xi_{bd}^0}{\partial x_{bf}} \right)_{\boldsymbol{x}_{sb}} \phi_q(\boldsymbol{\chi}_{sb}) \right) = 0 \quad \forall q \leq Q, f = 1, 2, \end{aligned} \quad (47)$$

$$\begin{aligned} \frac{\partial \chi^2}{\partial d_{gnf}} = & 2 \sum_s \sum_{b \neq g} w_{sgb} \sum_d (\xi_{gd}^0(\boldsymbol{x}_{ga}) - \xi_{bd}^0(\boldsymbol{x}_{sb}) + \\ & \sum_e \left( \frac{\partial \xi_{gd}^0}{\partial x_{ge}} \right)_{\boldsymbol{x}_{sg}} \left( \sum_p c_{pe} \phi_p(\boldsymbol{\chi}_{sg}) + \sum_m d_{gme} \psi_m(\boldsymbol{\chi}_{sg}) \right) - \\ & \sum_e \left( \frac{\partial \xi_{bd}^0}{\partial x_{be}} \right)_{\boldsymbol{x}_{sb}} \left( \sum_p c_{pe} \phi_p(\boldsymbol{\chi}_{sb}) + \sum_m d_{bme} \psi_m(\boldsymbol{\chi}_{sb}) \right)) \times \\ & \left( \frac{\partial \xi_{gd}^0}{\partial x_{gf}} \right)_{\boldsymbol{x}_{sg}} \psi_n(\boldsymbol{\chi}_{sg}) = 0 \quad \forall g, n \leq N, f = 1, 2, \end{aligned} \quad (48)$$

where  $Q$  is the number of free parameters  $c_{qf}$  and  $N$  is the number of free parameters  $d_{gnf}$  in each dimension  $f$  and for each field  $g$ . This leads to the normal equations

$$[\boldsymbol{\alpha}] \cdot \boldsymbol{c} = \boldsymbol{\beta}, \quad (49)$$

The  $[\boldsymbol{\alpha}]$  matrix can be decomposed in 4 sections with

$$\begin{aligned} \alpha_{qf, pe} = & \sum_s \sum_a \sum_{b>a} w_{sab} \sum_d \left( \left( \frac{\partial \xi_{ad}^0}{\partial x_{ae}} \right)_{\boldsymbol{x}_{sa}} \phi_p(\boldsymbol{\chi}_{sa}) - \left( \frac{\partial \xi_{bd}^0}{\partial x_{be}} \right)_{\boldsymbol{x}_{sb}} \phi_p(\boldsymbol{\chi}_{sb}) \right) \times \\ & \left( \left( \frac{\partial \xi_{ad}^0}{\partial x_{af}} \right)_{\boldsymbol{x}_{sa}} \phi_q(\boldsymbol{\chi}_{sa}) - \left( \frac{\partial \xi_{bd}^0}{\partial x_{bf}} \right)_{\boldsymbol{x}_{sb}} \phi_q(\boldsymbol{\chi}_{sb}) \right), \end{aligned} \quad (50)$$

$$\begin{aligned} \alpha_{gne, qf} = \alpha_{qf, gne} = & \sum_s \sum_{b \neq g} w_{sgb} \sum_d \left( \left( \frac{\partial \xi_{gd}^0}{\partial x_{gf}} \right)_{\boldsymbol{x}_{sg}} \phi_q(\boldsymbol{\chi}_{sg}) - \left( \frac{\partial \xi_{bd}^0}{\partial x_{bf}} \right)_{\boldsymbol{x}_{sb}} \phi_q(\boldsymbol{\chi}_{sb}) \right) \times \\ & \left( \frac{\partial \xi_{gd}^0}{\partial x_{ge}} \right)_{\boldsymbol{x}_{sg}} \psi_n(\boldsymbol{\chi}_{sg}), \end{aligned} \quad (51)$$

and

$$\alpha_{gqf,hne} = \sum_s w_{sgh} \sum_d \left( \frac{\partial \xi_{gd}^0}{\partial x_{gf}} \right)_{\boldsymbol{x}_{sg}} \psi_q(\boldsymbol{\chi}_{sg}) \times \left( \frac{\partial \xi_{hd}^0}{\partial x_{he}} \right)_{\boldsymbol{x}_{sh}} \psi_n(\boldsymbol{\chi}_{sh}). \quad (52)$$

The  $\beta$  vector has two sections:

$$\beta_{qe} = \sum_s \sum_a \sum_{b>a} w_{sab} \sum_d (\xi_{bd}^0(\boldsymbol{x}_{sb}) - \xi_{ad}^0(\boldsymbol{x}_{sa})) \times \left( \left( \frac{\partial \xi_{ad}^0}{\partial x_{af}} \right)_{\boldsymbol{x}_{sa}} \phi_q(\boldsymbol{\chi}_{sa}) - \left( \frac{\partial \xi_{bd}^0}{\partial x_{bf}} \right)_{\boldsymbol{x}_{sb}} \phi_q(\boldsymbol{\chi}_{sb}) \right), \quad (53)$$

and

$$\beta_{gqe} = \sum_s \sum_{b \neq g} w_{sgb} \sum_d (\xi_{bd}^0(\boldsymbol{x}_{sb}) - \xi_{gd}^0(\boldsymbol{x}_{sg})) \times \left( \frac{\partial \xi_{gd}^0}{\partial x_{ge}} \right)_{\boldsymbol{x}_{sg}} \psi_q(\boldsymbol{\chi}_{sg}). \quad (54)$$

## Appendix B

In the linear distortion case (`DISTORT_DEGREES 1`), the influence of the PV coefficients can be completely described by the standard WCS keywords `CDi_j` and `CRPIXi`. For the PV parameters, we have<sup>12</sup>:

$$x' = a_0 + a_1 x + a_2 y \quad (55)$$

$$y' = b_0 + b_1 y + b_2 x, \quad (56)$$

with

$$x = \text{CD1\_1}(X_1 - \text{CRPIX1}) + \text{CD1\_2}(X_2 - \text{CRPIX2}) \quad (57)$$

$$y = \text{CD2\_1}(X_1 - \text{CRPIX1}) + \text{CD2\_2}(X_2 - \text{CRPIX2}), \quad (58)$$

where the  $X_i$ s are the physical pixel coordinates. We want to express the  $x'$  and  $y'$  coordinates as a function of a new set of `CDi_j'` and `CRPIXi'` parameters:

$$x' = \text{CD1\_1}'(X_1 - \text{CRPIX1}') + \text{CD1\_2}'(X_2 - \text{CRPIX2}') \quad (59)$$

$$y' = \text{CD2\_1}'(X_1 - \text{CRPIX1}') + \text{CD2\_2}'(X_2 - \text{CRPIX2}'). \quad (60)$$

We find

$$\text{CD1\_1}' = a_1 \text{CD1\_1} + a_2 \text{CD2\_1} \quad (61)$$

$$\text{CD1\_2}' = a_1 \text{CD1\_2} + a_2 \text{CD2\_2} \quad (62)$$

$$\text{CD2\_1}' = b_1 \text{CD2\_1} + b_2 \text{CD1\_1} \quad (63)$$

$$\text{CD2\_2}' = b_1 \text{CD2\_2} + b_2 \text{CD1\_2}, \quad (64)$$

and

$$\text{CRPIX1}' = \text{CRPIX1} + \frac{b_0 \text{CD1\_2}' - a_0 \text{CD2\_2}'}{\text{CD1\_1}' \text{CD2\_2}' - \text{CD1\_2}' \text{CD2\_1}'} \quad (65)$$

$$\text{CRPIX2}' = \text{CRPIX2} + \frac{a_0 \text{CD2\_1}' - b_0 \text{CD1\_1}'}{\text{CD1\_1}' \text{CD2\_2}' - \text{CD1\_2}' \text{CD2\_1}'}. \quad (66)$$

---

<sup>12</sup><http://fits.gsfc.nasa.gov/registry/tpvwcs/tpv.html>